



Zn elemental and isotopic features in sinking particles of the South China Sea: Implications for its sources and sinks

Wen-Hsuan Liao^{a,1}, Shotaro Takano^b, Hung-An Tian^a, Hung-Yu Chen^c,
Yoshiki Sohrin^b, Tung-Yuan Ho^{a,d,*}

^a Research Center for Environmental Changes, Academia Sinica, Taipei, Taiwan

^b Institute for Chemical Research, Kyoto University, Uji, Japan

^c Department of Marine Environmental Informatics, National Taiwan Ocean University, Keelung, Taiwan

^d Institute of Oceanography, National Taiwan University, Taipei, Taiwan

Received 29 September 2020; accepted in revised form 10 September 2021; Available online 20 September 2021

Abstract

We determined the elemental and isotopic composition of Zn in sinking particles collected in the deep water of the northern South China Sea (NSCS) to investigate the relative contribution of various sources and assess their isotopic signatures. Using differentiable elemental ratios and $\delta^{66}\text{Zn}$ of the potential sources, a mass balance approach estimates that anthropogenic aerosol Zn accounted for $64 \pm 10\%$ of the total Zn in sinking particles for more than 50% of the sampling period, indicating that anthropogenic aerosol Zn has become a dominant form of Zn source in the deep water. A relatively large discrepancy between the estimated and measured $\delta^{66}\text{Zn}$ is observed during the high productivity season, which can be attributed to the elevated contribution of the biogenic hard parts or scavenging Zn on organic materials. Elevated $\delta^{66}\text{Zn}$ values were observed at 3500 m during autumn which may be caused by the influence of authigenic particles during the lowest flux period. We found that the averaged measured output $\delta^{66}\text{Zn}$ value, $+0.35 \pm 0.12\text{‰}$, is significantly lighter than most of the output values proposed in previous studies. Due to recent findings highlighting the importance of anthropogenic aerosol Zn in the ocean, we have re-evaluated the solubility and fluxes of aerosol Zn in the ocean and found that the flux has been significantly underestimated in previous studies. The updated global aerosol Zn input to the ocean, ranging from 0.3 to 3.0 Gmol yr^{-1} , is comparable to the output magnitude from hydrothermal and riverine sources. The updated Zn residence time would then be down to 1400 years on average. In addition to organic decomposition, the sinking particle data indicate that particle-associated removal and release processes play important roles in controlling Zn cycling in the water column. How anthropogenic aerosol deposition influences Zn fluxes and cycling in other oceanic regions deserves further investigation.

© 2021 Elsevier Ltd. All rights reserved.

Keywords: Zn isotopes; Anthropogenic aerosols; Sinking particles; SEATS; GEOTRACES

1. INTRODUCTION

Anthropogenic activities have considerably increased the input of biologically active elements on Earth and disturbed their natural cycling in the ocean. Among the various transport pathways of anthropogenic material to the ocean, aerosol deposition is considered a major pathway to deliver anthropogenic materials to the ocean (Chester

* Corresponding author at: Research Center for Environmental Changes, Academia Sinica, Taipei, Taiwan.

E-mail address: tyho@gate.sinica.edu.tw (T.-Y. Ho).

¹ Present address: UMR 6539/LEMAR/IUEM, CNRS, UBO, IRD, Ifremer, Technopôle Brest Iroise, Place Nicolas Copernic, Plouzané, France.

and Jickells, 2012b; Baker et al., 2016). Fossil fuel burning not only introduces CO₂ but also supplies a significant amount of anthropogenic aerosols to the ocean. Anthropogenic aerosol deposition provides a significant amount of reactive nitrogen species to surface waters of the North Pacific Ocean, which may potentially shift nutrient conditions from N-limited to P-limited in the North Pacific Ocean (Kim et al., 2014). Anthropogenic aerosols have also been reported to be an important source of trace metals (e.g., soluble Fe) to surface waters in some oceanic regions, and the impact of anthropogenic aerosol Fe may affect the entire ocean (Chuang et al., 2005; Sholkovitz et al., 2012; Ito et al., 2019). The elevated input of anthropogenic aerosol metals could significantly change trace metal bioavailability or toxicity in seawater for phytoplankton. How anthropogenic aerosol deposition has altered dissolved and particulate metal composition in the euphotic zone and their cycling mechanisms largely remains unknown.

The Northwestern Pacific Ocean (NWPO) and its marginal seas are right next to highly populated East Asia so that the oceanic regions have received tremendous amounts of anthropogenic aerosols during the past few decades (Wang et al., 2015). Two-thirds of the world's coal combustion was consumed in East Asia, providing a significant amount of anthropogenic aerosol Fe from coal-burning fly ashes to the surface ocean (Lin et al. 2015; Wang et al. 2015; Wang and Ho, 2020). In addition to aerosol Fe input, our studies have demonstrated that anthropogenic aerosol deposition can be a dominant source of many particulate trace metals in surface waters of the NWPO and its marginal seas (Ho et al., 2007; Liao et al., 2017; Liao and Ho, 2018). In the Western Philippine Sea, particulate trace metal to Al and to P ratios were found to be at least one order of magnitude higher than their lithogenic ratios and

intracellular quotas, implying that anthropogenic aerosols are a major trace metal source in the surface ocean (Liao et al., 2017). Similarly, previous studies demonstrated comparable patterns in the surface water at the Southeast Asia Time-series Study (SEATS) station in the northern South China Sea (NSCS, Fig. 1, Ho et al., 2007; Ho et al., 2010). In the deep water of the SEATS station, the elemental composition of sinking particles also suggested that some anthropogenic aerosol metals have been transported down to the deep water with sinking particles (Ho et al., 2011). In this study, the SEATS station was thus chosen to study the contribution of different sources on sinking particle metals in the deep water.

The major Zn inputs to the ocean include fluvial discharge, benthic and hydrothermal inputs, and aerosol deposition (Pacyna and Pacyna, 2001; Chester and Jickells, 2012a). It is worth noting that Zn has been massively used in various human activities, mainly including metallurgy, agriculture, energy production, microelectronics, sewage sludge, and scrap disposal. Among these activities, non-ferrous metal production and fossil fuel combustion account for roughly 85% of total anthropogenic aerosol Zn emissions globally (Pacyna and Pacyna, 2001). Zn is thus highly enriched in anthropogenic aerosols, generally with Zn to Al ratios to be at least two orders of magnitude higher than its crustal ratio (Chester and Jickells, 2012b). Furthermore, anthropogenic aerosol Zn possesses extremely high solubility, and Zn solubility in lithogenic aerosols is relatively low, typically less than 10% (Desboeufs et al., 2005; Shelley et al., 2018). In marine aerosols, previous studies reported that Zn solubility is usually higher than 70% for samples collected either in marginal seas or open oceans (Hsu et al., 2010; Chance et al., 2015; Shelley et al., 2018). High Zn solubility in anthropogenic aerosols

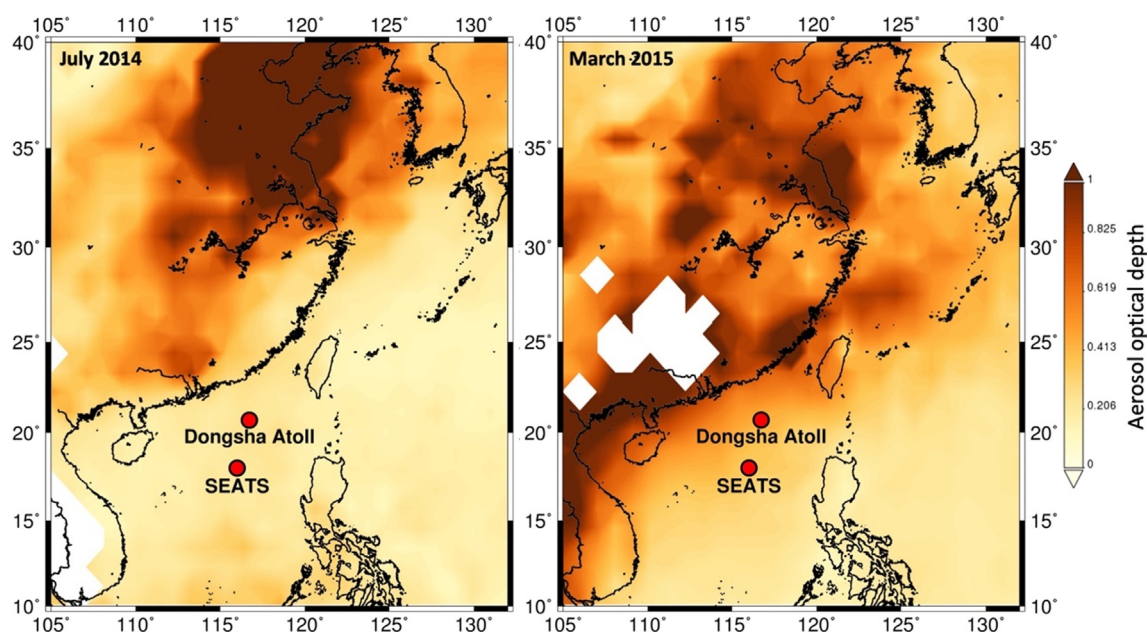


Fig. 1. The locations of the Southeastern Asian Time-series study (SEATS) station and the Dongsha Atoll (DS, 20°42'N 116°43'E) and monthly mean aerosol optical depth (AOD, dimensionless number) in July 2014 and March 2015 acquired from MODIS-Aqua at 550 nm (<http://giovanni.gsfc.nasa.gov>). The SEATS station is located at 18°N 116°E in the northern South China Sea with a bottom depth of 3783 m.

indicates that anthropogenic aerosol Zn is the dominant soluble Zn source in the surface ocean (Liao et al., 2020). Although the deposition fluxes of Zn from anthropogenic aerosols may be significant (Nriagu and Pacyna, 1988; Pacyna and Pacyna, 2001; Chester and Jickells, 2012a), its global quantitative contribution still remains unclear.

In addition to elemental ratios and solubility, Zn isotope composition ($\delta^{66}\text{Zn}$) offers specific information to investigate the sources and processes regulating Zn cycling in the marine water column (Conway and John, 2014; Little et al., 2014; Moynier et al., 2017). Previous studies reported that different Zn sources possess distinguishable $\delta^{66}\text{Zn}$ values, with lithogenic materials to be around +0.3‰ and anthropogenic materials to be generally lighter than lithogenic materials (Cloquet et al., 2006; John et al., 2007b; Chen et al., 2008; Rosca et al., 2019). In terms of seawater, dissolved $\delta^{66}\text{Zn}$ is around $+0.47 \pm 0.15\text{‰}$ in deep waters globally, but the surface value is generally isotopically lighter than the deep water in low and mid latitude regions (Bermin et al., 2006; Conway and John, 2014, 2015; John and Conway, 2014; John et al., 2017; Vance et al., 2019; Lemaître et al., 2020; Liao et al., 2020). Some studies have also reported different fractionation patterns in surface waters, which may be involved with other complicated processes, including external inputs or biological and physicochemical reactions in surface waters (John and Conway, 2014; Vance et al., 2019; Lemaître et al., 2020; Liao et al., 2020). Traditionally, lithogenic aerosols have been considered as the major source of aerosol Zn in the surface ocean. Recent studies suggested that the surface isotopically light $\delta^{66}\text{Zn}$ values can be attributed to scavenging or an important external Zn input, most likely to be anthropogenic aerosol deposition (Lemaître et al., 2020; Liao et al., 2020). Zn input originating from anthropogenic aerosol deposition in the marine water column deserves further investigation globally.

In terms of global Zn isotope budget, it is widely accepted that $\delta^{66}\text{Zn}$ in oceanic deep waters is constrained to an average value, $+0.47 \pm 0.15\text{‰}$ (Moynier et al., 2017). Riverine, aeolian, hydrothermal, and benthic inputs are considered to be the major sources and Fe-Mn deposits, carbonates, and siliceous sediments are the major sinks (Little et al., 2014; Moynier et al., 2017). The quantitative contribution and representative isotopic values of major inputs and outputs remain uncertain. A couple of studies argued that the $\delta^{66}\text{Zn}$ values of the major inputs to the global ocean are around +0.33‰, which are significantly lighter than the deep water $\delta^{66}\text{Zn}$ value (Little et al., 2014; Vance et al., 2016). These same studies also argued that the values of the major outputs are around +0.90‰, which are heavier than the deep water value. Little et al. (2014) thus proposed that an additional output with isotopically light Zn is needed to balance the budget under steady state assumption. However, based on model simulation, Weber et al. (2018) indicated that the burial Zn in the shelf regions accounts for over 90% of the total Zn output in the global ocean and the $\delta^{66}\text{Zn}$ of the output is $+0.36 \pm 0.04\text{‰}$, which is comparable to the value of the major inputs. Thus, the global Zn inputs and outputs can be balanced isotopically. Due to limited field observation and

model studies, we believe that it is still at an early stage to confirm representative values for the major inputs and outputs of Zn. It appears that field studies are needed to better assess the isotopic values of the major inputs and outputs in the ocean.

We determined Zn concentrations and isotope composition ($\delta^{66}\text{Zn}$) in sinking particles collected at 2000 and 3500 m at the SEATS station of the NSCS from April 2014 to March 2015 to evaluate the contribution of different Zn sources to the deep ocean. Using $\delta^{66}\text{Zn}$ and elemental ratios, we have quantified the contribution of anthropogenic aerosol Zn and other possible sources, including sediment resuspension and biogenic materials, in the deep water of the NSCS. To further assess the contribution of anthropogenic aerosol Zn to the global ocean, we have also re-examined all published information about major Zn inputs to the ocean and re-evaluated the importance of aerosol deposition to marine Zn cycling globally.

2. SAMPLING SITE AND METHODS

2.1. The oceanographic setting of the SEATS station

The sampling site, SEATS station, was established in 1999 as a part of time series studies in the Joint Global Ocean Flux Study (JGOFS) by Taiwan to investigate the cycling of carbon and other bioactive major elements in the South China Sea (Fig. 1). A sediment trap program was carried out and maintained since 2003 to study material fluxes and cycling at SEATS (Wong et al., 2007; Lui et al., 2018). Due to the elevated mixing induced by the winter monsoon in the NSCS (Tseng et al., 2005; Pan et al., 2015; Lui et al., 2018), primary production peaks in winter and results in a relatively high material sinking flux in the oceanic region. Significant amount of lithogenic and anthropogenic materials originating from East Asia are transported by the winter monsoon to the NSCS during winter and spring (Lin et al., 2007; Lin et al., 2015). Previous studies have shown that anthropogenic aerosols originated from East Asia may be a critical source of trace metals in the surface and deep water of the SCS (Ho et al., 2007; Ho et al., 2010; Ho et al., 2011). The SEATS station is also located in an oceanic region with high fluvial input, mainly from the Pearl River. Lateral transport may be a source of materials in the oceanic region. Furthermore, the well-studied physical condition of the NSCS provides us sufficient information to quantify the relative contribution of lateral transport and physical mixing on material cycling in the NSCS (Yang et al., 2012; Liao et al., 2020).

2.2. Sampling of sinking particles

Time-series moored sediment traps were deployed at the SEATS station at 2000 and 3500 m on two occasions. The first deployment lasted from 15 April 2014 to 16 October 2014; the second one from 21 November 2014 to 4 March 2015. French time-series sediment traps (Technicap Pièges à Particules Séquentiels, models 5/2) were used to collect sinking particles, with 1.00 m² cone area and 8-day collection interval for each cup. The trap body and baffle material

were made of reinforced polyester and phenolic composite, respectively. Polypropylene trapping bottles (Nalgene) were acid washed before use. Trap solution was prepared by adding 800 g of Merck guarantee reagent grade NaCl to 20 liters of subsurface seawater taken near the trap deployment location where dissolved Zn concentrations were below 1 nM in the surface water of the NSCS (Wen et al., 2006; Ho et al., 2011; Yang et al., 2012). As the total amounts of trace metals in the sinking particles collected in the traps were at least two orders of magnitude higher than those originating from the NaCl salts, contamination from the trap solution is negligible. After retrieving the traps, the sample bottles were detached, sealed, and stored in a cold room at 4 °C onboard until further processing in land based laboratory.

2.3. Sampling of size-fractionated aerosols

Aerosol samples were collected at Dongsha island, a coral reef atoll near SEATS (Fig. 1). The samples of PM 2.5 (particle size less than 2.5 µm aerodynamic diameter) and PM 2.5–10 were collected by a low-volume dichotomous sampler (Thermo Andersen SA-241) with flow rate of 16.7 L min⁻¹ on a daily basis from January to December 2010. The aerosol filters used were pre-weighed PTFE membrane filters (37 mm diameter, 1 µm pore size). Aerosol Zn concentrations on the filters were generally two to three orders of magnitude higher than the background Zn concentrations of the filter blanks. In detail, the Zn concentration or mass of the blank is 1.51 ± 0.45 nmol L⁻¹ or 0.48 ± 0.14 ng (n = 5), and the ones for samples ranges from 112 to 5482 nmol L⁻¹ or 36 to 1754 ng (summer to winter, low to high flux season).

2.4. Determination of elemental concentration

All sample preparation work was carried out in flow benches with Ultra Low Particulate Air (ULPA) filtration within a class 100 clean room at Research Centre of Environmental Changes, Academia Sinica. Ultrapure reagents were purchased from the manufacturer (Seastar or J. T. Baker). The pretreatment procedures of elemental concentrations in sinking particle and aerosol samples were similar. Prior to inductively coupled plasma mass spectrometer (ICPMS) analysis, one eighth of the sinking particle samples were obtained from the original trapping bottles. We filtered the samples onto weighted 0.2 µm polycarbonate (PC) membranes (Whatman) and rinsed them by Milli-Q to remove seawater residue. After freeze-drying, the samples were weighed. For aerosol samples, half of each filter (37 mm PTFE membrane) was used for trace metal analysis. Both the sinking particle and aerosol samples were digested with a 5 mL mixture of concentrated ultrapure HNO₃ and HF in 15 mL PFA vials (Savillex) at 120 °C for 12 hrs on a hot plate in a laminar flow bench of a clean laboratory. The digestion solution was then evaporated to dryness on a hot plate in a trace-metal clean hood. Subsequently, the dried samples were further digested by a 5 mL mixture of concentrated ultrapure HNO₃ and HCl to fully digest all materials. The digested solution was

evaporated to dryness. The samples were then re-dissolved in 1 mL concentrated ultrapure HNO₃ and was evaporated to dryness again. The dried samples were re-dissolved and diluted by using 0.5 M ultrapure HNO₃ for trace metal analysis by ICPMS. All reported elemental concentrations were analyzed by a sector field high resolution ICPMS (Thermo Fisher Scientific, Element XR), which was carried out using a SC-Fast autosampler (Elemental Scientific) and an Apex HF (Elemental Scientific). Reference materials, HISS-1 (marine sediment; National Research Council Canada) and BCR-414 (river plankton; European Commission), were also digested by the same procedures mentioned above to check precision and validate accuracy. The deviations of measured trace metal concentrations from the certified values are all better than 10%. The details of the precision, accuracy, and detection limits of the methods were described in previous studies (Ho et al., 2011; Liao et al., 2017; Takano et al., 2020).

2.5. Zn isotope composition measurement

The Zn isotope composition in sinking particles and aerosols was measured by using a new method for samples containing lithogenic particles (Takano et al. 2020), which is modified from a previous study for seawater samples (Takano et al., 2017). The fractions of Ni, Cu, and Zn in the sinking particle sample were obtained by the same column chemistry experiments carried out in the study of Takano et al. (2020). Prior to isotopic analysis, based on the concentrations obtained by ICPMS, all samples were quantitatively spiked with a ⁶⁴Zn-⁶⁷Zn double spike solution with a spike to sample ratio of 1. Some elements, such as Al, Ti, and Fe, in the samples would cause isotopic interferences during analysis, such as ²⁷Al³⁷Cl⁺ on ⁶⁴Zn. We have thus developed a method by modifying the procedure of Nobias Chelate-PA1 chelate extraction to remove Fe, Al, and Ti in the samples. A Poly-Prep open column (Bio-Rad) loaded with ~ 360 mg of the Nobias Chelate-PA1 resin was used to preconcentrate trace metals. Solutions were passed through the column by gravity. In the pre-concentration procedure, a solution of 1.6 M NH₄F prepared by ultrapure grade ammonium hydroxide and HF, adjusted to pH 5 by 0.03 M acetate buffer, was passed through the resins to eliminate Fe, Al, and Ti prior to trace metal elution. After trace metal extraction, the Zn fraction was further purified by using AG-MP1 anion exchange resin. Detailed procedures of this modified method are shown in Table 1 and the study of Takano et al. (2020). The procedural blanks of Zn were 0.62 ± 0.35 and 0.31 ± 0.29 ng for Nobias PA1 preconcentration and AG-MP1 purification, respectively. The overall procedural blank of Zn was 0.92 ± 0.46 ng. The interference caused by the blank mass is negligible on Zn isotope measurement as the general sample masses were around 200 ng. The averaged digestion recovery of Zn was $103 \pm 10\%$, which was obtained from three different certified reference materials (Table 2).

Zn isotope compositions were measured by a multi-collector ICP-MS (Thermo Fisher Scientific, Neptune plus) at the Institute of Earth Sciences, Academia Sinica. Samples and standards were introduced by a Teflon PFA

Table 1
Trace metal extraction and anion exchange procedures used in this study.

Trace metal extraction procedure ^a		
Step	Eluent	Volume (mL)
Clean	1 M HNO ₃	5
	Ultrapure water	5
Condition	0.05 M Buffer (pH 5)	4
Loading	Sample (pH 5)	X ^b
Remove Al, Ti, Fe	1.6 M NH ₄ F (pH 5)	5
Remove prior solution	Milli-Q	12
Trace metal Elution	1 M HNO ₃	5
Clean	1 M HNO ₃	3
	Ultrapure water	3
Anion exchange procedure ^c		
Step	Eluent	Volume (mL)
Clean	1 M HNO ₃	3
Condition	4 M HCl	1.6
Sample loading	4 M HCl	0.9
Elution of Ni, Ti, Cu	4 M HCl	3
Elution of Fe and Mo	1 M HCl	3.5
Elution of Zn	1 M HNO ₃	2.5

^a The Poly-Prep prepacked gravity flow column (Bio-Rad) was used here and the bed volume of trace metal extraction column is 0.6 mL, ~360 mg Nobias Chelate-PA1 resin.

^b The sample was dissolved in a 1 mL mixture solution of 0.5 M HNO₃ and 0.01 M HF and it was adjusted to pH 4.7–5.2 by using the acetate buffer.

^c The 5 mL Teflon columns (Savillex) and HDPE frits were used here and the bed volume of the anion exchange column is roughly 0.56 mL.

nebulizer and an Apex-IR desolvation system (ESI) at 100 $\mu\text{L min}^{-1}$, with Ni X-type skimmer and H-type sampler cones. Medium-resolution mode was used to resolve Zn from polyatomic interferences (ArAl⁺ and ArNO⁺). Signal intensities were measured for atomic masses 62, 64, 66, 67, and 68 with ⁶²Ni used to correct for isobaric interferences of ⁶⁴Ni to ⁶⁴Zn, and further details can be found in these studies (Takano et al., 2017; 2020). Zn isotope ratios were calculated using a double-spike data reduction scheme based on the iterative approach of Siebert et al. (2001), and all ratios were expressed relative to JMC-Lyon to compare with previous data sets. Each sample was analyzed twice, and the average isotopic ratios are reported. Error estimation of Zn isotope composition was based on the method described in Conway et al. (2013). The reproducibility of Zn isotope ratio has been checked by repeating the measurement of IRMM-3702, $+0.27 \pm 0.05$ ($n > 200$), which was identical to the reported value, $+0.30 \pm 0.06$

Table 2
Zn concentrations and isotopic composition of reference materials ($n = 3$).

	Measured Concentration ($\mu\text{g/g}$)	Consensus value ($\mu\text{g/g}$)	$\delta^{66}\text{Zn}$ (Ave \pm 2SE ^a)	Reference $\delta^{66}\text{Zn}$ values
BHVO-2	108 \pm 2	112 \pm 3	0.35 \pm 0.06	0.28 \pm 0.04 ^b
BCR-2	102 \pm 1	103 \pm 6	0.28 \pm 0.07	0.25 \pm 0.03 ^b
NIES-28	145 \pm 15	127 \pm 9	0.06 \pm 0.07	-

^a Two-standard error in MC-ICP-MS measurement.

^b The $\delta^{66}\text{Zn}$ values of the certified reference materials, BHVO-2 and BCR-2, were reported in Moynier et al. (2017).

(Moynier et al., 2017; Liao et al., 2020). The accuracy of Zn isotope analysis in our laboratory has been examined by an intercomparison study shown in Liao et al. (2020), and we also measured three different certified reference materials for accuracy validation (Table 2).

3. RESULTS

3.1. The mass, elemental fluxes, and Zn isotope composition of sinking particles

The mass fluxes of sinking particles exhibit significant seasonal patterns at the SEATS station. The mass fluxes at 2000 and 3500 m gradually decrease from May to November ranging from 150 to 20 $\text{mg m}^{-2} \text{d}^{-1}$, then increased dramatically to 300 ~ 400 $\text{mg m}^{-2} \text{d}^{-1}$ in winter and early spring (Fig. 2a). The mass fluxes of sinking particles showed a close relationship with the satellite-derived chlorophyll-*a* concentrations, an indicator of the amount of biogenic materials produced in the euphotic zone (Lui et al., 2018). The relationship indicates that the mass fluxes of sinking particles are mainly driven by primary production at the SEATS station (Tseng et al., 2005; Liu et al., 2013; Lui et al., 2018). The elemental fluxes of Zn, P, and Al in the sinking particles are shown in Fig. 2b, c, and d. The fluxes of these three elements show similar seasonal patterns, with some relatively high values observed in winter and spring and the lowest value observed in summer. Vertically, the fluxes of these three elements were generally at the same order of magnitude at the two depths. For Zn, the fluxes at 3500 m were higher than at 2000 m in September and October, and one abrupt increase was found in February. For Al, the fluxes at 3500 m were higher than at 2000 m particularly from July to September, but the fluxes at 2000 m were higher than at 3500 m in January. In terms of P fluxes, the amplitude of its seasonal variation was similar to the mass flux, with some high values observed in the winter and early spring (Fig. 2a and c). The 2000 m fluxes of P are significantly higher than at 3500 m during winter and early spring. The fluxes at 2000 m in January were elevated for all three elements.

Elemental ratios, Zn to P and Zn to Al, are calculated and compared with the reference ratios in lithogenic material and plankton intracellular Zn quota (Ho et al., 2003; Hu and Gao, 2008; Liao et al., 2017) (Fig. 2e and f). In general, the Zn to Al ratios were significantly higher than the lithogenic ratios and the Zn to P ratios were one to two orders of magnitude higher than the intracellular Zn quota. At 3500 m, the two ratios were elevated from September to October, which is attributed to the elevated Zn fluxes

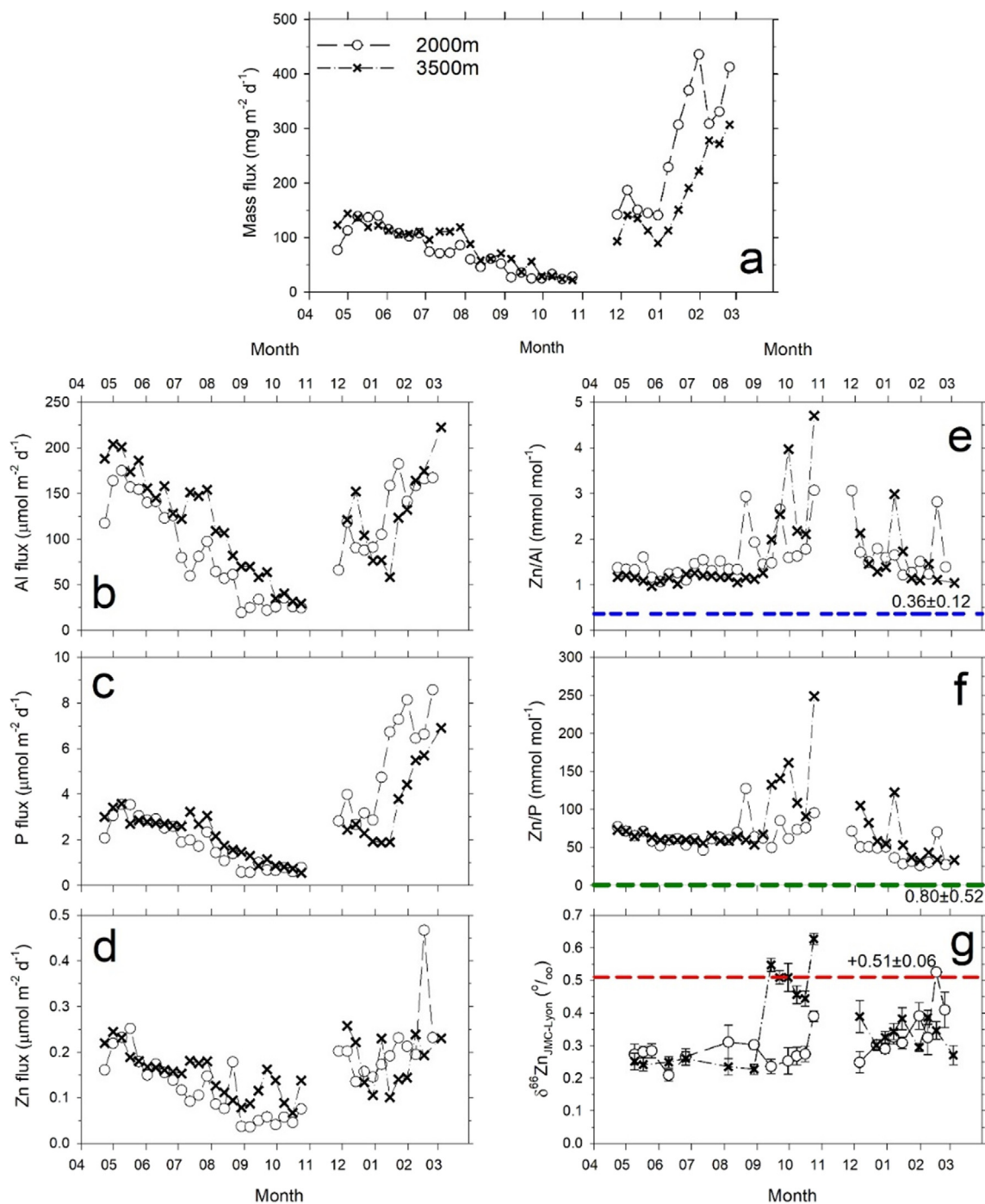


Fig. 2. The temporal variations of mass fluxes, elemental fluxes (Al, P, and Zn), elemental ratios (Zn/Al and Zn/P), and Zn isotope composition ($\delta^{66}\text{Zn}$) of the sinking particles. The open circles and cross symbols represent the data obtained at 2000 m and 3500 m, respectively. The green dash line represents the Zn/P quota and the blue line stands for the lithogenic Zn/Al ratio (compiled in Liao et al., 2017). The red dash line represents the lithogenic $\delta^{66}\text{Zn}$ values reported near the SEATS station (Bentahila et al., 2008).

(Fig. 2d). In terms of Zn isotope composition, the $\delta^{66}\text{Zn}$ values are roughly around +0.30‰ for most of the sampling time. The temporal variation of $\delta^{66}\text{Zn}$ is relatively small from May to August. We observed some elevated $\delta^{66}\text{Zn}$ values at 3500 m with the value ranging from +0.40 to +0.64‰ in September and October, concurrent with the lowest Al, P, and total mass fluxes (Fig. 2a, b, and c).

4. DISCUSSION

4.1. Seasonal Changes of masses and elemental fluxes of sinking particles

Early studies have found that the northeastern monsoon, occurring from October to April, is the major driving

force causing seasonal changes of primary production in the NSCS (Tseng et al., 2005; Pan et al., 2015; Lui et al., 2018). Specifically, the elevated primary production is attributed to the coupling effect of relatively high temperature (22 to 24 °C) and increasing nutrient supply by water mixing in the euphotic zone. The elevated biomass would result in high mass fluxes of sinking particles in the water column, particularly in winter and spring seasons (Lui et al., 2018). This unique seasonal pattern observed at the SEATS station is opposite to the Hawaii Ocean Time-series (HOTS) station, a time series station in the oligotrophic North Pacific Subtropical Gyre. The primary production at the HOTS station generally peaks in summer (Karl et al., 2021). In addition to inducing elevated primary production in winter and spring seasons, the monsoon also transports aerosols originating from East Asia to the NSCS (Lin et al., 2007; Lin et al., 2015).

Our previous study also reported year round sinking particle data collected in 2004 and 2005 at the same studied site (Ho et al., 2011). Here, we have compiled and exhibited the seasonal patterns of elemental fluxes, particularly at 3500 m (Fig. 3). As expected, relatively high mass fluxes were observed during winter and spring seasons for the two sampling occasions (Fig. 3a). In terms of the low flux seasons, which were from September to early November, the mass fluxes in 2004 and 2005 were significantly higher than 2014. We found that the overall seasonal patterns of Al and Zn fluxes were comparable among the two occasions. However, P fluxes were significantly different among the two periods, with P fluxes in 2004 and 2005 being two-fold higher in the high aerosol flux seasons and 5-fold

higher in the low flux seasons than the ones in 2014 and 2015. These results suggest that the intracellular Zn portion and Zn from lithogenic particles seem to account for a minor fraction of total particulate Zn in the sinking particles.

4.2. The contribution of different Zn sources in sinking particles

In terms of the total mass of sinking particles, biogenic and lithogenic particles are two major components (Tan et al., 2020; Zhang et al., 2019). In addition to biogenic and lithogenic materials, our previous studies found that anthropogenic aerosol Zn is a dominant Zn source in sinking particles not only in the surface water but also in the deep water of the NSCS (Ho et al., 2007; Ho et al., 2010; Ho et al., 2011). Zn to Al ratios in aerosols collected in the NSCS are generally two orders of magnitude higher than the ratios in lithogenic materials (Liao et al., 2017). In addition to elemental ratios, $\delta^{66}\text{Zn}$ ratios in anthropogenic aerosols are lower than in lithogenic materials (Moynier et al., 2017; Rosca et al., 2019). The $\delta^{66}\text{Zn}$ values of biogenic hard parts and Fe-Mn oxides are all around +1.0‰, with $\delta^{66}\text{Zn}$ ranging from +0.81 to +1.34‰ for carbonate shell, from +0.70 to +1.50‰ for diatom frustules, and from +0.70 to +1.06‰ for Fe-Mn oxides in the Pacific Ocean, which are all higher than lithogenic materials (Maréchal et al., 2000; Pichat et al., 2003; Andersen et al., 2011).

Other than external sources, internal cycling processes, mainly including biological uptake, scavenging, particle

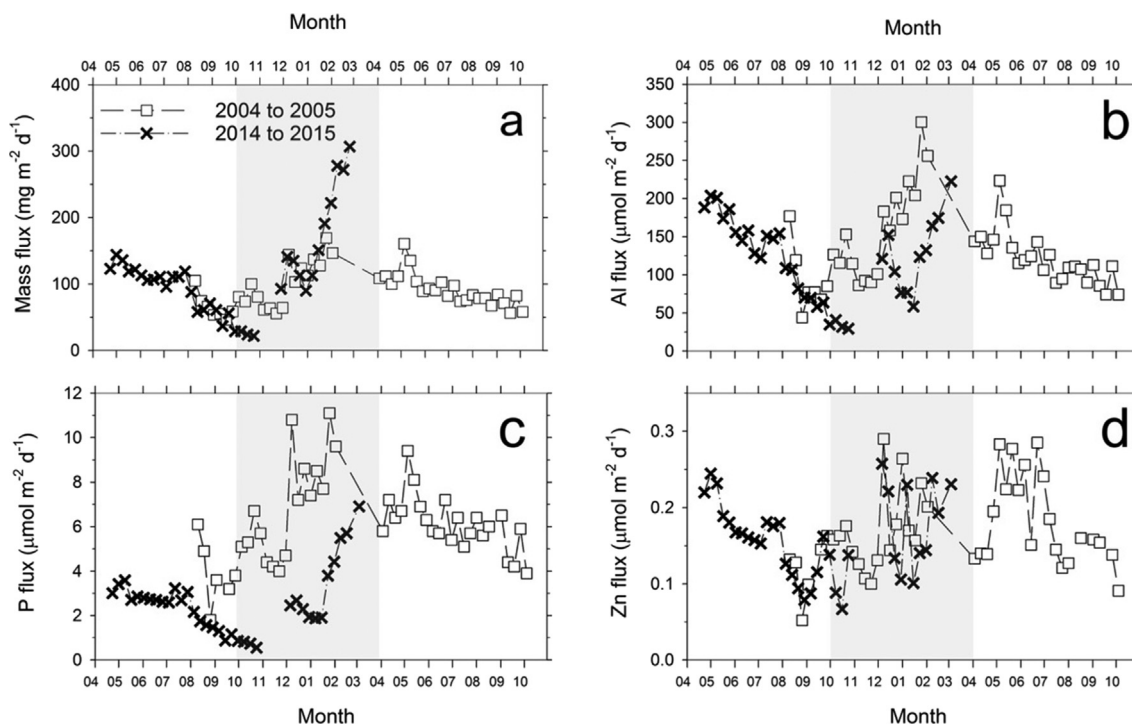


Fig. 3. The comparison of masses and elemental fluxes at 3500 m in two collection periods, 2004 to 2005 (Ho et al. 2011) and 2014 to 2015 (this study). The grey area represents the occurrence of the northeastern monsoon from October to April.

aggregation, and authigenic particle precipitation, may also change the elemental and isotopic composition of sinking particles. For example, adsorption of anthropogenic aerosol metals on suspended or sinking particles is highly likely to increase Zn to Al ratios in the particles (Ho et al., 2011). Some studies have demonstrated that adsorption of Zn onto degrading phytoplankton or biofilms tends to scavenge relatively heavy Zn from seawater (John et al., 2007a; Coutaud et al., 2014; John and Conway, 2014). On the other hand, laboratory culture experiments have observed that marine diatoms take up isotopically light Zn relative to the medium, with 0.2 to 0.4‰ difference between phytoplankton and the medium (John et al., 2007a; Köbberich and Vance, 2017, 2018; Samanta et al., 2018). The Zn isotope fractionation of aggregation and authigenic particles precipitation still remains unknown. How these internal cycling processes alter the elemental and isotopic composition of trace metals in sinking particles still remains unclear. In this study, by assuming that elemental and isotopic composition of the sinking particles are mainly decided by external sources, we may then apply elemental and isotopic ratios to evaluate the quantitative contribution of the major sources for trace metals in the sinking particles.

Our previous studies in the NSCS have found that lithogenic, biogenic, and anthropogenic components may explain the majority of the variability of elemental composition for most of the trace metals determined in suspended particles (e.g., Ho et al. 2007; 2010; 2011; Liao and Ho, 2018). Since sinking particles originate from suspended particles, we may first assume that Zn in sinking particles mainly originates from lithogenic, biogenic, and anthropogenic components. We then use the reference elemental ratios to estimate the contribution of the three components as we did in the previous studies. By assuming that Al is all from lithogenic materials and the lithogenic Zn to Al ratio is 0.36 mmol mol⁻¹ (Hu and Gao, 2008), the estimated lithogenic Zn fraction accounts for 24 and 27% on average in sinking particles collected at 2000 and 3500 m, respectively, with values ranging from 12 to 34% and 8 to 37% of total Zn (Eq. (1); Fig. 4a and b). The estimated lithogenic fractions in this study were within the range estimated by a previous study at SEATS during 2004 and 2005, which ranged from 20 to 62% at 3500 m (Figure 8 of Ho et al. (2011)).

The biogenic component in sinking particles contains hard (CaCO₃ and biogenic silica) and soft parts (particulate organic matter). The molar ratios of Zn/Ca and Zn/Si in hard parts were 3.2 and 7.5 μmol mol⁻¹, respectively (Andersen et al., 2011; Marchitto et al., 2000). Using the reported elemental ratios and the mass fluxes of hard parts measured at SEATS, Zn abundance in hard parts only accounted for 1% of the total Zn mass in sinking particles at SEATS. Although CaCO₃ and biogenic silica fractions generally accounted for over half of the total mass flux measured in this study, Zn in hard parts can be ignored in our mass balance calculation. The biogenic organic fraction accounted for roughly 10% of the total mass fluxes (Tan et al., 2020). This soft part, biogenic organic fraction, may be further separated into intracellular Zn by biological uptake and extracellular Zn by scavenging process.

Operationally, since we cannot separate these two fractions in our mass balance calculation, we thus use an apparent Zn/P ratio, 5.5 ± 2.0 mmol mol⁻¹, observed in the surface water of the NSCS to present the biogenic organic fraction (Ho et al., 2007). The NSCS averaged value is also comparable to the global averaged value, 5.8 ± 4.5 mmol mol⁻¹ (data compiled in Table 4 of Liao et al., 2017). Although we do not have the seasonal Zn/P values in the NSCS to evaluate the seasonal variations, the sensitivity test using the lower and upper limits of the Zn/P range observed in the NSCS (Ho et al. 2007), 3.5 and 7.5 mmol mol⁻¹, showing that the variations of the ratio range only accounts for 4% of total Zn mass at most.

Assuming that Zn in sinking particles mainly originates from lithogenic, biogenic, and anthropogenic aerosol materials, we may input the known information of individual fraction and isotopic composition of the three components to the following equations to compare the estimated value with the observed ones to validate the importance of anthropogenic aerosol Zn.

$$F_{\text{litho}} = R_{\text{litho}}[\text{Al}]_{\text{total}}/[\text{Zn}]_{\text{total}} \quad (1)$$

$$F_{\text{bio}} = R_{\text{bio}}[\text{P}]_{\text{total}}/[\text{Zn}]_{\text{total}} \quad (2)$$

$$F_{\text{litho}} + F_{\text{bio}} + F_{\text{an}} = 1 \quad (3)$$

$$F_{\text{litho}} \delta^{66}\text{Zn}_{\text{litho}} + F_{\text{bio}} \delta^{66}\text{Zn}_{\text{bio}} + F_{\text{an}} \delta^{66}\text{Zn}_{\text{an}} = \delta^{66}\text{Zn}_{\text{calculated}} \quad (4)$$

where F_{litho} : the fraction of lithogenic Zn

F_{bio} : the fraction of organic biogenic Zn, including intracellular and adsorbed Zn

F_{an} : the fraction of anthropogenic aerosol Zn

R_{litho} : lithogenic Zn to Al ratio of 0.36 mmol mol⁻¹

R_{bio} : apparent biogenic Zn to P ratio of 5.5 mmol mol⁻¹ observed in the NSCS

$\delta^{66}\text{Zn}_{\text{litho}}$: Zn isotope composition of lithogenic Zn

$\delta^{66}\text{Zn}_{\text{bio}}$: Zn isotope composition of biogenic Zn

$\delta^{66}\text{Zn}_{\text{an}}$: Zn isotope composition of the anthropogenic aerosol Zn

The fraction information of each component can be calculated from the first three equations (Fig. 4a and b). The biogenic Zn fraction accounted for 11 and 9% of total Zn on average in sinking particles collected at 2000 and 3500 m, respectively, with values ranging from 5 to 22% and 2 to 18% of total Zn temporally (Eq. (2); Fig. 4a and b). Based on mass balance, the anthropogenic Zn fraction can account for 64% of total Zn on average at both 2000 and 3500 m, with values ranging from 46 to 83% and 47 to 90% of total Zn temporally (Eq. (3)).

For the isotope composition in the lithogenic term, studies suggested that lithogenic particles originating from Taiwan is the largest sediment source in the NSCS (Liu et al., 2016). The lithogenic $\delta^{66}\text{Zn}$ values in the sediment core collected at Manila Trench and from Taiwan's rocks were +0.52 ± 0.06 and +0.50 ± 0.06‰, respectively (Bentahila et al., 2008). We thus use the averaged value of the two data sets, +0.51 ± 0.06‰, as a representative $\delta^{66}\text{Zn}$ of lithogenic materials in the formula. In terms of the $\delta^{66}\text{Zn}$ value in the biogenic organic component, we assume that the value obtained in the component of the

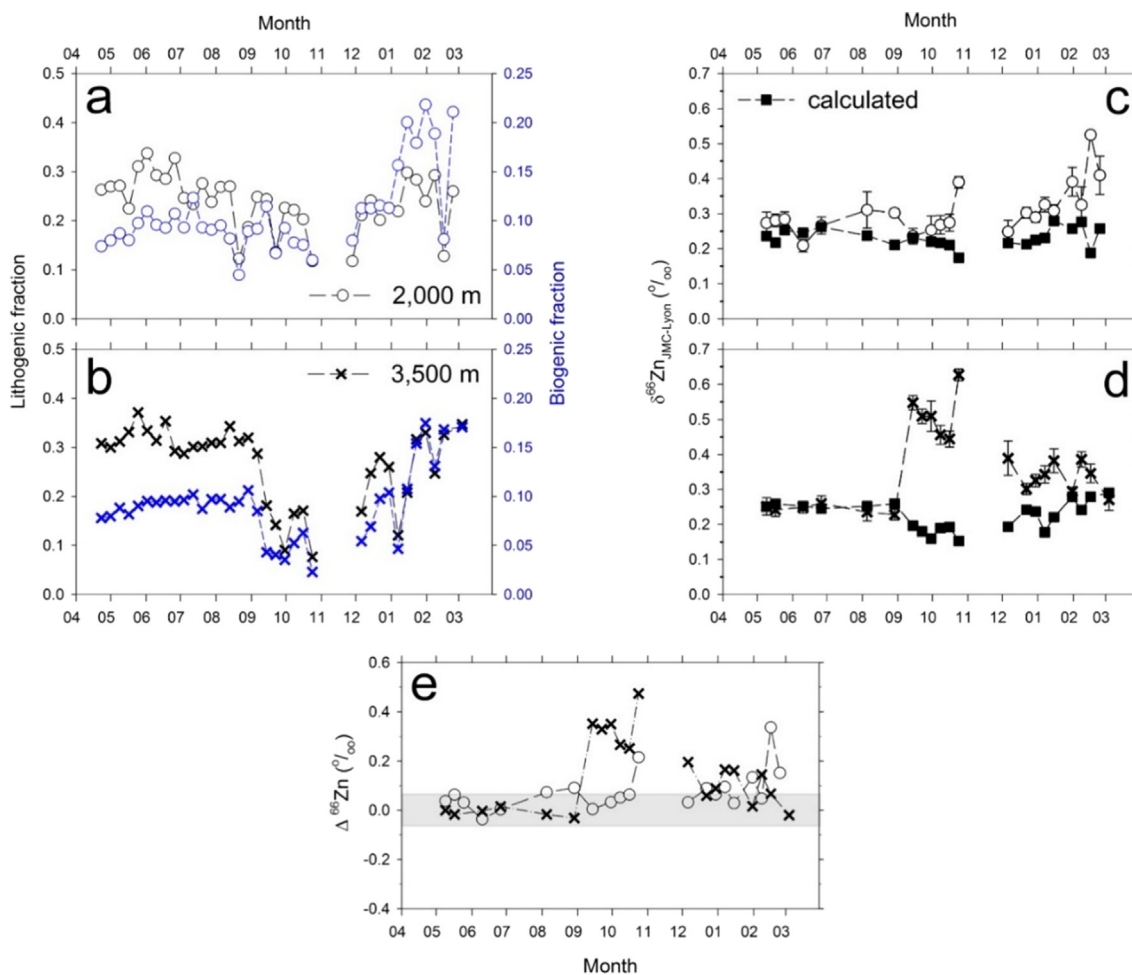


Fig. 4. The temporal variations of estimated lithogenic and biogenic Zn portions in the sinking particles collected at 2000 (a) and 3500 m (b) from April 2014 to March 2015. The open circles and cross symbols represent the data obtained at 2000 m and 3500 m, respectively. Black and blue symbols in panel a and b represent the lithogenic and biogenic Zn portions, respectively. The comparison of the calculated and measured $\delta^{66}\text{Zn}$ values of sinking particles collected at 2000 (c) and 3500 m (d), respectively. The discrepancy of the calculated and measured $\delta^{66}\text{Zn}$ ($\Delta^{66}\text{Zn}$) was shown in panel e. The gray bar stands for the typical external error of Zn isotope measurement, $\pm 0.06\text{‰}$, obtained in Zn isotope related studies.

deep water is comparable to the $\delta^{66}\text{Zn}$ observed in the surface water, where the sinking particles are mainly composed of biogenic materials (Ho et al., 2007). Our previous studies showed that the $\delta^{66}\text{Zn}$ values in the sinking particles collected in the surface waters of two different oceanic regions, the NSCS and the Western Philippine Sea, were close to each other, which were $+0.16 \pm 0.08$ ($n = 11$) and $+0.17 \pm 0.06\text{‰}$ ($n = 12$), respectively (Liao, 2019). The variations of the $\delta^{66}\text{Zn}$ values observed at different depths in the surface water of the Western Philippine Sea were statistically insignificant, which were $+0.16 \pm 0.06$, $+0.19 \pm 0.06$, and $+0.14 \pm 0.13\text{‰}$ for 50, 150, 300 m, respectively (Liao, 2019). Assuming no significant fractionation with remineralization during sinking processes over the depth, we thus use the averaged value obtained in the surface water to represent the value in the deep water. The $\delta^{66}\text{Zn}$ value, $+0.17\text{‰}$, can thus be considered as an averaged value of the biogenic fraction, including intracellular and extracellular adsorbed Zn. In terms of $\delta^{66}\text{Zn}$ in anthropogenic aerosols, we have obtained the average $\delta^{66}\text{Zn}$ values of

size-fractionated aerosol samples collected at the Dongsha Atoll, which were $+0.16 \pm 0.12$ and $+0.072 \pm 0.065$ for PM 2.5 ~ 10 and PM 2.5 aerosols, respectively (Table 3). The values obtained at the Dongsha Atoll is close to the $\delta^{66}\text{Zn}$ value of anthropogenic aerosols reported previously, ranging from $+0.10$ to $+0.30\text{‰}$ (Cloquet et al., 2006; John et al., 2007b). We thus use the average value of all aerosol $\delta^{66}\text{Zn}$ measured in this study, $+0.12 \pm 0.10\text{‰}$, as the $\delta^{66}\text{Zn}$ value of anthropogenic aerosol Zn at SEATS (Table 3). Based on the mass balance assumption with known fraction information and the representative $\delta^{66}\text{Zn}$ of the three components shown in Eq. (4), the calculated $\delta^{66}\text{Zn}$ values of sinking particles are compared with the measured values in Fig. 4.

The comparison of the calculated and measured $\delta^{66}\text{Zn}$ values and their discrepancy ($\Delta^{66}\text{Zn}$) is shown in Fig. 4c, d, e. The discrepancy of 22 points, out of 42 samples, between the measured and calculated $\delta^{66}\text{Zn}$ values is smaller than the typical external error of Zn isotope measurement, $\pm 0.06\text{‰}$. These low and analytically insignif-

Table 3

Zn isotope composition in the size-fractionated aerosols collected at Dongsha Atoll in the NSCS (Fig. 1).

Date	PM2.5			PM2.5 ~ 10		
	nmol m ⁻³	$\delta^{66}\text{Zn}$	2SE*	nmol m ⁻³	$\delta^{66}\text{Zn}$	2SE*
2011/5/12	4.84	0.08	0.04	0.53	0.08	0.05
2011/6/10	0.72	0.17	0.05	0.57	0.44	0.05
2011/6/27	4.47	0.18	0.04	0.63	0.11	0.04
2011/7/21	n.d.			0.62	0.11	0.05
2011/7/27	1.17	0.08	0.04	0.48	0.10	0.04
2011/8/5	2.20	0.12	0.04	0.55	0.21	0.04
2011/8/13	0.52	0.05	0.03	n.d.		
2011/8/20	2.69	0.03	0.05	0.34	0.19	0.05
2011/8/21	2.53	0.04	0.04	0.34	0.07	0.05
2011/9/14	2.64	0.06	0.04	n.d.		
2011/12/20	13.5	-0.04	0.05	n.d.		

* The standard error of $\delta^{66}\text{Zn}$ values represents the instrumental precision of Zn isotope measurement of each sample.

Table 4

Zn solubility in different aerosol types.

Aerosol type	Location	Particle size (μm)	Zn solubility (%)	
Lithogenic dust	Loess of Cape Verde ^a	2–20	11	
	Arizona dust ^a	0.6–12	13	
Urban aerosols	S. California ^b	< 8	68	
	Porcheville Fly-Ash ^a	< 100	99	
	Vitry Fly-Ash ^a	2–100	19	
Marine aerosols	Urban particulate matter ^a	0.03–10	100	
	Corsica ^c	> 0.4	72	
	GCE ^d	> 0.2	99	
	North Sea ^e	< 35	58	
		< 20	72	
		< 20	75	
	Ireland ^f	< 20	73	
		> 0.2	96	
		Bermuda ^f	> 0.2	96
		Gulf of Aqaba ^g	> 0.2	44
		East China Sea ^h	< 20	84
Southeastern Atlantic ⁱ		< 20	72	
North Atlantic Ocean ^j		< 20	55	
Arctic Ocean ^k	< 20	51		

^a Desboeufs et al. (2005),^b Hodge et al. (1978),^c Losno et al. (1988),^d Lim and Jickells (1990),^e Chester et al. (1994); Chester et al. (1993); Kersten et al. (1991),^f Lim et al. (1994),^g Chen et al. (2006),^h Hsu et al. (2010),ⁱ Chance et al. (2015),^j Shelley et al. (2018),^k Kadko et al. (2019).

icant discrepancy indicate that our approach can be a good first order estimate of $\delta^{66}\text{Zn}$ values in sinking particles for half of the time and validate that our assumptions on the isotopic value shown in the Eq. (4) are reasonable. Most importantly, the results support that anthropogenic aerosol Zn accounted for a major fraction of Zn in the sinking particles, $64 \pm 10\%$. The dissolved $\delta^{66}\text{Zn}$ values at the SEATS ranged from +0.26 to +0.41‰ at depths from 1800 to 3650 m, which are slightly lower than the global deep water

averaged value, $+0.47 \pm 0.15\%$ (Liao et al. 2020). These results indicate that sinking particles transport light Zn originating from anthropogenic aerosols to the deep water of the SEATS station.

Although the assumption may not fully explain all trap data, the assumption does explain a majority of the variation of the data set. Indeed, for a few unique months with extremely low fluxes, the three-component assumption is insufficient but useful to deduce an unknown source with

a relatively heavy isotopic composition. Some relatively large $\Delta^{66}\text{Zn}$ values were observed at both depths (Fig. 4e). At 3500 m, elevated $\delta^{66}\text{Zn}$ values were observed from September to October (autumn) with $\Delta^{66}\text{Zn}$ values ranging from +0.27 to +0.50‰. Relatively large $\Delta^{66}\text{Zn}$ values were also observed from December to February (winter) for both depths, with the values mostly ranging from +0.09 to +0.17‰. As pointed out in the Result section, the total mass fluxes increased significantly during winter (Fig. 2a). Although the biogenic inorganic Zn fraction may only account for 1% of total Zn on average, its contribution may increase 3 to 4 folds to around 3 to 4% during winter. Indeed, a previous study reported that the abundance of both coccolithophore and diatom was much higher in winter than summer in the NSCS (Chen, 2005). The diatom frustules and siliceous materials possess a relatively high $\delta^{66}\text{Zn}$, ranged from +0.70 to +1.50‰ (Andersen et al., 2011; Hendry and Andersen, 2013). Similarly, Zn from CaCO_3 shells was isotopically heavy, with an average value to be $+0.91 \pm 0.47\text{‰}$ (Pichat et al., 2003). Using the similar isotopic mass balance approach, the contribution of hard fraction may induce an increase of $\delta^{66}\text{Zn}$ around +0.03 to 0.04‰ during winter.

In addition to increase of the hard part Zn component, particulate P also increased around threefold during winter (Fig. 2c). On average, organic biogenic Zn fraction also increased by twofold during winter (Fig. 4a and b). The increasing input of organic matter coupled with internal cycling processes may be a potential factor causing the relatively high discrepancy during winter. Some internal cycling processes involved, such as scavenging, may also increase $\delta^{66}\text{Zn}$ in sinking particles. Supported by culture experiments and model studies, scavenging of heavy Zn onto particles can be an important process in fractionating Zn in the ocean, especially in deep waters, where the adsorbed Zn plays a much dominant role than biogenic Zn (John et al., 2007a; John and Conway, 2014; Weber et al., 2018). Thus, scavenging of heavy Zn onto biogenic particles may be the other possible cause of isotopically heavy Zn in the sinking particles. In brief, the isotopically heavy values observed in winter were possibly attributed to the elevated biogenic hard and soft parts during the period.

The other discrepancy was observed from September to October (autumn) at 3500 m, with $\Delta^{66}\text{Zn}$ ranging from +0.27 to +0.50‰ (Fig. 3d). We found that all elemental and isotopic ratios showed abnormally high values at 3500 m during the autumn period (Fig. 2e, f, and g). We also found that the fluxes of total mass, Al, and P were the lowest during the whole sampling period for both depths (Fig. 2a, b, and c) and the estimated fractions of lithogenic and biogenic Zn were the lowest in the whole studied period at 3500 m (Fig. 4b). However, Zn fluxes at 3500 m were about twofold higher than the values observed at 2000 m during the autumn period (Fig. 2e). The patterns of these parameters suggest that there was an additional particulate Zn source with relatively high $\delta^{66}\text{Zn}$ at 3500 m during the period. Authigenic minerals can be a potential candidate for the isotopically heavy Zn anomaly. For example, ferromanganese oxides, which possess high Zn/Al

ratios and isotopically heavy composition (Maréchal et al., 2000; Little et al., 2014), may be the particulate Zn source. Indeed, a previous study at the same study site observed elevated Mn fluxes and Mn to Al ratios at 3500 m and suggested that authigenic Mn oxides originating from lateral transport were the major source of the elevated Mn flux (Ho et al., 2011). The authigenic particles may be laterally transported from the continental shelf to the offshore region by the effect of mesoscale eddies in deep waters (Adams et al., 2011). It appears that the relative contribution of the unknown fraction, likely to be authigenic minerals, on $\delta^{66}\text{Zn}$ would become significant during the lowest mass flux period. It should be noted that the Zn contribution from the authigenic fraction only accounted for a minor portion of the total particulate Zn mass annually (Fig. 4b). In addition to the two obvious discrepancies mentioned above, a slight increase in August–September and a spike in February–March were also observed at 2000 m (Fig. 4c and e). These elevated $\delta^{66}\text{Zn}$ values seem to correspond to a significant drop of both biogenic and lithogenic fractions (Fig. 4a), which may also be explained by the increasing percentage of authigenic particles with isotopically heavy Zn. Overall, the mass balance estimate supports the importance of anthropogenic aerosol Zn in the deep ocean of the NSCS. Anthropogenic aerosol Zn is a dominant source of particulate Zn not only in the surface water but also in the deep water of the NSCS.

4.3. Implications for the global marine Zn isotope budget

As mentioned in the introduction, based on limited field observation and model studies (Little et al., 2014; Weber et al., 2018), we think that it is still at an early stage to confirm representative values for the major marine inputs and outputs of Zn to carry out the global isotopic mass balance calculation. More field studies should be conducted to get representative values for the major marine inputs and outputs of Zn. In terms of sinking particle studies, only one study reported relatively light $\delta^{66}\text{Zn}$ values at 2500 m in the Central Atlantic Ocean, with an average value of $+0.24 \pm 0.05\text{‰}$ (Maréchal et al., 2000). This study shall provide valuable information to assess the Zn output and budget in the global ocean.

The Zn fluxes observed at 3500 m in this study ranged from 2.4×10^{-5} to $9.4 \times 10^{-5} \text{ mol m}^{-2} \text{ yr}^{-1}$, with an average value of $5.8 \times 10^{-5} \text{ mol m}^{-2} \text{ yr}^{-1}$. The observed fluxes in this study are at the same order of magnitude to the model derived burial rates in the NSCS (Weber et al., 2018), roughly ranging from 10^{-4} to $10^{-5} \text{ mol m}^{-2} \text{ yr}^{-1}$. The model derived burial $\delta^{66}\text{Zn}$ in the deep ocean ranged from +0.40 to +0.70‰ with an average value of +0.64‰ (Weber et al., 2018). However, our flux-weighted average $\delta^{66}\text{Zn}$ in the 3500 m sinking particles was $+0.35 \pm 0.12\text{‰}$. This value was significantly lighter than the model derived burial $\delta^{66}\text{Zn}$ values, suggesting that the isotopically light aerosol Zn may also increase the amount of the light Zn output, particularly in the high aerosol flux seasons. In our dataset, some relatively heavy $\delta^{66}\text{Zn}$ values were observed in the low aerosol flux seasons, ranging from +0.44

to +0.64‰, which are close to the model derived average value (+0.64‰). The seasonal variations observed from our data reflect that the relatively heavy values are highly likely caused by the extremely low input of anthropogenic aerosols. In addition to anthropogenic aerosol input, riverine Zn may be a significant anthropogenic source. Two previous studies reported that Zn originating from anthropogenic activities was an important source of riverine Zn, which accounted for 70% of the particulate Zn pool in the riverine water (Chen et al., 2008; Chen et al., 2009). The impacts of anthropogenic origin Zn on the global oceanic Zn budget deserve more studies.

4.4. Impact of anthropogenic aerosol Zn on the modern oceanic Zn mass balance

The importance of anthropogenic aerosols as a major Zn source in the ocean may be beyond marginal seas. Our recent study indicated that anthropogenic aerosol Zn input may be an important source causing dissolved $\delta^{66}\text{Zn}$ to be isotopically light in most of the surface water of the NWPO and aerosol deposition is also closely related to dissolved Zn concentrations in surface waters of the oceanic regions with high aerosol optical depth (Liao et al., 2020). One recent study in the North Atlantic Ocean also pointed out the importance of anthropogenic aerosols in determining $\delta^{66}\text{Zn}$ in the surface water (Lemaitre et al., 2020). However, lithogenic aerosols are traditionally considered to be the major source of aerosol Zn in the global ocean. Using total lithogenic aerosol input in the ocean and assuming the aerosol Zn solubility to be 15%, Little et al. (2014) estimated the global aerosol soluble Zn flux to be $0.069 \text{ Gmol yr}^{-1}$, which is about one order of magnitude lower than the averaged riverine Zn flux, $0.59 \text{ Gmol yr}^{-1}$. The contribution of anthropogenic aerosol Zn input to the global ocean should be reevaluated. In terms of Zn solubility in aerosols, it has been widely observed that the solubility of anthropogenic aerosol Zn is much higher than the solubility of lithogenic aerosol Zn (Desboeufs et al., 2005). Intriguingly, we found that Zn solubility in marine aerosols is generally high in various major open oceans and marginal seas (Table 4), indicating the significant quantitative contribution of anthropogenic aerosols in marine aerosols. We thus think that anthropogenic aerosols are the dominant soluble Zn source in marine aerosols globally due to high Zn solubility, high Zn enrichment factor, and relatively fine sizes of aerosols.

Taking stock of current published datasets about aerosol Zn flux and Zn solubility in the ocean, we have reevaluated the range of the global marine aerosol soluble Zn flux and compared it with the other two major sources, riverine and hydrothermal inputs (Table 4, Fig. 5). Zn concentrations in marine aerosols generally ranged from 0.1 to 20 ng m^{-3} (Witt et al., 2010; Liao and Ho, 2018; Shelley et al., 2018). Zn solubility of marine aerosols ranged from 44 to 99% (Table 4). Using the low end of aerosol Zn concentration range reported by the three studies mentioned above, 0.1 to 1 ng m^{-3} , the average Zn solubility to be 70% (Table 4), assuming the dry Zn aerosol deposition rate to be 0.3 cm s^{-1} (Chance et al., 2015), and the wet to dry

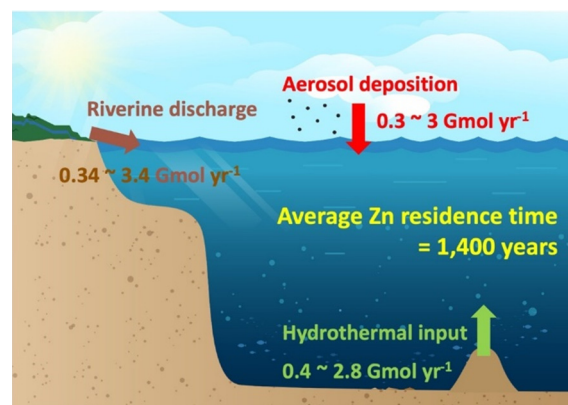


Fig. 5. The comparison of the fluxes of three major Zn inputs to the ocean, including riverine, aerosol, and hydrothermal inputs. The oceanic Zn inventory is 7.2 Tmol , estimated by the average dissolved Zn concentration (5.4 nM), global ocean area ($3.6 \times 10^{14} \text{ m}^2$), and the average depth of the ocean (3700 m).

deposition ratio to be 7 (Ho et al., 2010; Chance et al., 2015), the global oceanic aerosol Zn deposition flux would range from 0.3 to 3.0 Gmol yr^{-1} . The uncertainty of the flux can be up to one order of magnitude. Duce et al. (1991) also obtained a comparable atmospheric Zn flux to the ocean, ranging from 0.7 to 3.5 Gmol yr^{-1} .

Global riverine fluxes should also be re-evaluated. Although Gaillardet et al. (2003) comprehensively compiled published riverine Zn concentrations globally and estimated the average Zn concentration to be $0.6 \mu\text{g L}^{-1}$, most of global major rivers have been seriously polluted by anthropogenic activities during the past two decades (Zhou et al., 2020). For example, the riverine Zn concentrations reported in Amazon basin and Changjiang ranged from 2 to 8.5 and from 0.43 to $49 \mu\text{g L}^{-1}$, respectively (Wen et al., 2013; Guinoiseau et al., 2018), which are at least one order of magnitude higher than the value reported by Gaillardet et al. (2003). Using the global riverine mass discharge flux, $3.7 \times 10^{16} \text{ kg yr}^{-1}$ (Dai and Trenberth, 2002) and concentrations ranging from 0.6 to $6 \mu\text{g L}^{-1}$ (Gaillardet et al., 2003; Wen et al., 2013; Guinoiseau et al., 2018), the estimated riverine Zn input flux to the ocean would then range from 0.34 to 3.4 Gmol yr^{-1} . Using a similar approach, Chester and Jickells (2012a) estimated the flux to be 7.2 Gmol yr^{-1} . In terms of the global hydrothermal Zn input in the ocean, a few recent studies estimated the flux to range from 0.4 to 2.8 Gmol yr^{-1} by using measurements of excess Zn in hydrothermal plumes of the southeastern Pacific Ocean coupled with an estimate of hydrothermal ^3He inputs (Roshan et al., 2016; Holzer et al., 2017; Roshan et al., 2018). The flux estimated by Elderfield and Schultz (1996) also ranges from 1.2 to 3.2 Gmol yr^{-1} . The flux ranges of the three major sources to the ocean are at the same order of magnitudes (Fig. 5). Aerosols may play an even more important role to surface waters of the open ocean than the other two sources due to its ease for long distance transport to surface waters.

Reported oceanic Zn residence times have shown a large uncertainty, ranging from 1100 to $50,000$ years (Shiller and Boyle, 1985; Bruland et al., 1994; Little et al., 2014; Roshan

et al., 2016; Hayes et al., 2018). Assuming riverine flux as the dominant Zn source, the residence times estimated were as long as 11,000 or 50,000 years (Shiller and Boyle, 1985; Little et al., 2014). By using a scavenging removal approach, the time ranged from 3000 to 6000 years (Bruland et al., 1994); by using hydrothermal Zn as the dominant input, the residence time was 3000 ± 600 years (Roshan et al., 2016). Using the ^{232}Th approach, the residence time can be as low as 1100 ± 600 years (Hayes et al., 2018). Based on the steady state assumption of dissolved Zn concentrations and the updated three major flux data (Fig. 5), the residence time we have estimated ranges from 750 to 7000 years, with an average to be 1400 years. The estimated Zn residence times of these recent studies (Roshan et al., 2016; Hayes et al., 2018) are significantly shorter than major nutrients, which is at the levels of several ten thousand years (e.g., Benitez-Nelson, 2000; Tréguer and De La Rocha, 2013). Some recent studies show that Zn cycling processes in the global ocean are more complicated than major nutrients. In addition to biological uptake and physical mixing (Vance et al., 2017; Middag et al., 2019), scavenging process and external sources may play significant roles in regulating Zn cycling in the ocean (Vance et al., 2017; Weber et al., 2018; Middag et al., 2019).

In addition to physical mixing and scavenging processes, this study indicates that the external Zn input may be a critical factor causing the variation of Zn concentrations and its isotopic composition in the marine water column. In contrast to the comparable Cd to P ratios in the deep water of the Pacific Ocean, we found that Zn to P ratios exhibit an increasing trend from the Southern Ocean to the North Pacific Ocean. The Cd to P ratios at depth deeper than 1500 m were 0.35 ± 0.02 ($n = 60$), 0.32 ± 0.02 ($n = 348$), and 0.35 ± 0.02 ($n = 219$) mmol mol^{-1} in the Southern Ocean, the South Pacific Ocean, and the North Pacific Ocean, respectively (Schlitzer et al., 2018; Zheng et al., 2021). The ratios of dissolved Zn to P were 2.49 ± 0.40 ($n = 42$), 3.12 ± 0.37 ($n = 332$), and 3.70 ± 0.21 ($n = 134$) mmol mol^{-1} in the three oceanic regions from the south to the north (Zheng et al., 2021), respectively. The increasing trend of Zn/P ratios is possibly related to the external inputs to the North Pacific Ocean. Some other studies also pointed out the potential importance of external sources for dissolved Zn cycling in the North Pacific Ocean. Based on the spatial variations of Zn elemental or isotopic composition, it has been proposed that sedimentary input from the continental margins of the North Pacific Ocean may be a potential dissolved Zn source in deep waters (Conway and John, 2015). Our previous study also observed elevated Zn concentrations in surface waters of the North Pacific Ocean and found that surface Zn concentrations possess a positive relationship with aerosol optical depth globally, indicating the importance of aerosol Zn input on Zn cycling in the water column (Liao et al., 2020). Aerosol Zn input coupled with scavenging process may be a critical factor causing Zn to be elevated in the deep ocean of the North Pacific Ocean. How external sources influence oceanic Zn internal cycling and interact with scavenging and physical mixing deserves further investigation, especially in the Pacific Ocean.

5. CONCLUSION

We determined Zn concentrations and $\delta^{66}\text{Zn}$ in sinking particles collected at 2000 and 3500 m of the SEATS station in the NSCS to study Zn biogeochemical cycling processes and budget in the marine water column. We found that anthropogenic aerosol Zn was the dominant source of Zn in sinking particles, which accounted for $64 \pm 10\%$ of the total Zn mass on average for longer than 50% of the sampling period. The significant contribution may explain the low $\delta^{66}\text{Zn}$ value observed in the sinking particles, $+0.35 \pm 0.12\text{‰}$. This value was significantly lower than the $\delta^{66}\text{Zn}$ output values reported in previous studies, suggesting that the isotopically light aerosol Zn may increase the amount of the light Zn output. Based on the updated global fluxes of major Zn inputs, the marine Zn residence time estimated is around 1400 years on average, shorter than the one of major nutrients. In addition to internal cycling processes, the external Zn input may play a critical role in influencing marine Zn cycling. How marine Zn cycling is regulated by the interaction between internal cycling processes and external inputs deserves to be studied further.

Declaration of Competing Interest

The authors declare that they have no known competing financial interests or personal relationships that could have appeared to influence the work reported in this paper.

ACKNOWLEDGEMENT

We acknowledge the personnel of TORI for deploying and recovering the sediment trap mooring system, especially to S.-H. Ho, B.-S. Wang, F. Kuo, C.-J. Tseng, and H.-L. Lin. We thank the captains and crew of the R/V Ocean Researchers I, III and V for their assistance during the related cruises. We thank W.-C. Tu, C.-C. Hsieh, and K.-F. Huang for their technical support and S.-C. Yang, K.-F. Huang, P. Lam, G.T. F. Wong, and C.-L. Wei for providing helpful comments on this manuscript. We also thank N. Llopis Monferrer for preparing Fig. 5. We thank two anonymous reviewers and the associate editor, Claudine Stirling, for their constructive comments, which have significantly improved the quality of our manuscript. This study was mainly supported by Taiwan Ministry of Science and Technology grants 105-2119-M-001-039-MY3 and 108-2611-M-001-006-MY3, the Investigator Award of T.-Y. Ho from the Academia Sinica, and partially by ICR-iJURC Short-term Exchange Program to S. Takano, and the International Collaborative Research Program of Institute for Chemical Research, Kyoto University.

APPENDIX A. SUPPLEMENTARY DATA

Supplementary data to this article can be found online at <https://doi.org/10.1016/j.gca.2021.09.013>.

REFERENCES

- Adams D. K., McGillicuddy D. J., Zamudio L., Thurnherr A. M., Liang X., Rouxel O., German C. R. and Mullineaux L. S. (2011) Surface-Generated Mesoscale Eddies Transport Deep-Sea Products from Hydrothermal Vents. *Science* **332**, 580–583.

- Andersen M. B., Vance D., Archer C., Anderson R. F., Ellwood M. J. and Allen C. S. (2011) The Zn abundance and isotopic composition of diatom frustules, a proxy for Zn availability in ocean surface seawater. *Earth Planet. Sci. Lett.* **301**, 137–145.
- Baker, A.R., Landing, W.M., Bucciarelli, E., Cheize, M., Fietz, S., Hayes, C.T., Kadko, D., Morton, P.L., Rogan, N., Sarthou, G., Shelley, R.U., Shi, Z., Shiller, A. and van Hulst, M.M.P., 2016. Trace element and isotope deposition across the air-sea interface: progress and research needs. *Philos. Trans. A Math. Phys. Eng. Sci.* 374.
- Benitez-Nelson C. R. (2000) The biogeochemical cycling of phosphorus in marine systems. *Earth Sci. Rev.* **51**, 109–135.
- Bentahila, Y., Ben Othman, D. and Luck, J.-M., 2008. Strontium, lead and zinc isotopes in marine cores as tracers of sedimentary provenance: A case study around Taiwan orogen. *Chem. Geol.* **248**, 62–82.
- Bermin J., Vance D., Archer C. and Statham P. J. (2006) The determination of the isotopic composition of Cu and Zn in seawater. *Chem. Geol.* **226**, 280–297.
- Bruland K. W., Orians K. J. and Cowen J. P. (1994) Reactive trace metals in the stratified central North Pacific. *Geochim. Cosmochim. Acta* **58**, 3171–3182.
- Chance R., Jickells T. D. and Baker A. R. (2015) Atmospheric trace metal concentrations, solubility and deposition fluxes in remote marine air over the south-east Atlantic. *Mar. Chem.* **177**, 45–56.
- Chen J., Gaillardet J. and Louvat P. (2008) Zinc isotopes in the Seine River waters, France: a probe of anthropogenic contamination. *Environ. Sci. Technol.* **42**, 6494–6501.
- Chen J., Gaillardet J., Louvat P. and Huon S. (2009) Zn isotopes in the suspended load of the Seine River, France: Isotopic variations and source determination. *Geochim. Cosmochim. Acta* **73**, 4060–4076.
- Chen, Y.-I.L., 2005. Spatial and seasonal variations of nitrate-based new production and primary production in the South China Sea. *Deep Sea Research Part I: Oceanogr. Res. Papers* **52**, 319–340.
- Chen Y., Street J. and Paytan A. (2006) Comparison between pure-water- and seawater-soluble nutrient concentrations of aerosols from the Gulf of Aqaba. *Mar. Chem.* **101**, 141–152.
- Chester R., Bradshaw G. F. and Corcoran P. A. (1994) Trace metal chemistry of the North Sea particulate aerosol; concentrations, sources and sea water fates. *Atmos. Environ.* **28**, 2873–2883.
- Chester R. and Jickells T. (2012a) The Transport of Material to the Oceans: Relative Flux Magnitudes, *Marine Geochemistry. John Wiley & Sons Ltd*, 92–124.
- Chester R. and Jickells T. (2012b) The Transport of Material to the Oceans: The Atmospheric Pathway, *Marine Geochemistry. John Wiley & Sons Ltd*, 52–82.
- Chester R., Murphy K. J. T., Lin F. J., Berry A. S., Bradshaw G. A. and Corcoran P. A. (1993) Factors controlling the solubilities of trace metals from non-remote aerosols deposited to the sea surface by the 'dry' deposition mode. *Mar. Chem.* **42**, 107–126.
- Chuang P. Y., Duvall R. M., Shafer M. M. and Schauer J. J. (2005) The origin of water soluble particulate iron in the Asian atmospheric outflow. *Geophys. Res. Lett.* **32**, n/a-n/a.
- Cloquet C., Carignan J. and Libourel G. (2006) Isotopic Composition of Zn and Pb Atmospheric Depositions in an Urban/ Periurban Area of Northeastern France. *Environ. Sci. Technol.* **40**, 6594–6600.
- Conway T. M. and John S. G. (2014) The biogeochemical cycling of zinc and zinc isotopes in the North Atlantic Ocean. *Global Biogeochem. Cycles* **28**, 1111–1128.
- Conway T. M. and John S. G. (2015) The cycling of iron, zinc and cadmium in the North East Pacific Ocean – Insights from stable isotopes. *Geochim. Cosmochim. Acta* **164**, 262–283.
- Conway T. M., Rosenberg A. D., Adkins J. F. and John S. G. (2013) A new method for precise determination of iron, zinc and cadmium stable isotope ratios in seawater by double-spike mass spectrometry. *Anal. Chim. Acta* **793**, 44–52.
- Coutaud A., Meheut M., Viers J., Rols J.-L. and Pokrovsky O. S. (2014) Zn isotope fractionation during interaction with phototrophic biofilm. *Chem. Geol.* **390**, 46–60.
- Dai A. and Trenberth K. E. (2002) Estimates of Freshwater Discharge from Continents: Latitudinal and Seasonal Variations. *J. Hydrometeorol.* **3**, 660–687.
- Desboeufs K. V., Sofikitis A., Losno R., Colin J. L. and Ausset P. (2005) Dissolution and solubility of trace metals from natural and anthropogenic aerosol particulate matter. *Chemosphere* **58**, 195–203.
- Duce R. A., Liss P. S., Merrill J. T., Atlas E. L., Buat-Menard P., Hicks B. B., Miller J. M., Prospero J. M., Arimoto R., Church T. M., Ellis W., Galloway J. N., Hansen L., Jickells T. D., Knap A. H., Reinhardt K. H., Schneider B., Soudine A., Tokos J. J., Tsunogai S., Wollast R. and Zhou M. (1991) The atmospheric input of trace species to the world ocean. *Global Biogeochem. Cycles* **5**, 193–259.
- Elderfield H. and Schultz A. (1996) Mid-Ocean Ridge Hydrothermal Fluxes and the Chemical Composition of the Ocean. *Annu. Rev. Earth Planet. Sci.* **24**, 191–224.
- Gaillardet J., Viers J. and Dupré B. (2003) 5.09 - Trace Elements in River Waters. In *Treatise on Geochemistry* (eds. H. D. Holland and K. K. Turekian). Pergamon, Oxford, pp. 225–272.
- Guinoiseau D., Bouchez J., Gélabert A., Louvat P., Moreira-Turcq P., Filizola N. and Benedetti M. F. (2018) Fate of particulate copper and zinc isotopes at the Solimões-Negro river confluence, Amazon Basin, Brazil. *Chem. Geol.* **489**, 1–15.
- Hayes C. T., Anderson R. F., Cheng H., Conway T. M., Edwards R. L., Fleisher M. Q., Ho P., Huang K.-F., John S. G., Landing W. M., Little S. H., Lu Y., Morton P. L., Moran S. B., Robinson L. F., Shelley R. U., Shiller A. M. and Zheng X.-Y. (2018) Replacement Times of a Spectrum of Elements in the North Atlantic Based on Thorium Supply. *Global Biogeochem. Cycles* **32**, 1294–1311.
- Hendry K. R. and Andersen M. B. (2013) The zinc isotopic composition of siliceous marine sponges: Investigating nature's sediment traps. *Chem. Geol.* **354**, 33–41.
- Ho T.-Y., Chou W.-C., Lin H.-L. and Sheu D. D. (2011) Trace metal cycling in the deep water of the South China Sea: The composition, sources, and fluxes of sinking particles. *Limnol. Oceanogr.* **56**, 1225–1243.
- Ho T.-Y., Chou W.-C., Wei C.-L., Lin F.-J., Wong G. T. F. and Lin H.-L. (2010) Trace metal cycling in the surface water of the South China Sea: Vertical fluxes, composition, and sources. *Limnol. Oceanogr.* **55**, 1807–1820.
- Ho T.-Y., Quigg A., Finkel Z. V., Milligan A. J., Wyman K., Falkowski P. G. and Morel F. M. M. (2003) The elemental composition of some marine phytoplankton. *J. Phycol.* **39**, 1145–1159.
- Ho T.-Y., Wen L.-S., You C.-F. and Lee D.-C. (2007) The trace metal composition of size-fractionated plankton in the South China Sea: Biotic versus abiotic sources. *Limnol. Oceanogr.* **52**, 1776–1788.
- Hodge V., Johnson S. R. and Goldberg E. D. (1978) Influence of atmospherically transported aerosols on surface ocean water composition. *Geochem. J.* **12**, 7–20.
- Holzer M., DeVries T., Bianchi D., Newton R., Schlosser P. and Winckler G. (2017) Objective estimates of mantle ³He in the

- ocean and implications for constraining the deep ocean circulation. *Earth Planet. Sci. Lett.* **458**, 305–314.
- Hsu S.-C., Wong G. T. F., Gong G.-C., Shiah F.-K., Huang Y.-T., Kao S.-J., Tsai F., Candice Lung S.-C., Lin F.-J., Lin I. I., Hung C.-C. and Tseng C.-M. (2010) Sources, solubility, and dry deposition of aerosol trace elements over the East China Sea. *Mar. Chem.* **120**, 116–127.
- Hu Z. and Gao S. (2008) Upper crustal abundances of trace elements: A revision and update. *Chem. Geol.* **253**, 205–221.
- Ito A., Myriokefalitakis S., Kanakidou M., Mahowald N. M., Scanza R. A., Hamilton D. S., Baker A. R., Jickells T., Sarin M., Bikina S., Gao Y., Shelley R. U., Buck C. S., Landing W. M., Bowie A. R., Perron M. M. G., Guieu C., Meskhidze N., Johnson M. S., Feng Y., Kok J. F., Nenes A. and Duce R. A. (2019) Pyrogenic iron: The missing link to high iron solubility in aerosols. *Science. Advances* **5**, eaau7671.
- John S. G. and Conway T. M. (2014) A role for scavenging in the marine biogeochemical cycling of zinc and zinc isotopes. *Earth Planet. Sci. Lett.* **394**, 159–167.
- John S. G., Geis R. W., Saito M. A. and Boyle E. A. (2007a) Zinc isotope fractionation during high-affinity and low-affinity zinc transport by the marine diatom *Thalassiosira oceanica*. *Limnol. Oceanogr.* **52**, 2710–2714.
- John S. G., Genevieve Park J., Zhang Z. and Boyle E. A. (2007b) The isotopic composition of some common forms of anthropogenic zinc. *Chem. Geol.* **245**, 61–69.
- John S. G., Helgoe J. and Townsend E. (2017) Biogeochemical cycling of Zn and Cd and their stable isotopes in the Eastern Tropical South Pacific. *Mar. Chem.*
- Kadko D., Aguilar-Islas A., Bolt C., Buck C. S., Fitzsimmons J. N., Jensen L. T., Landing W. M., Marsay C. M., Rember R., Shiller A. M., Whitmore L. M. and Anderson R. F. (2015) The residence times of trace elements determined in the surface Arctic Ocean during the 2015 US Arctic GEOTRACES expedition. *Mar. Chem.* **208**(2019), 56–69.
- Karl D. M., Letelier R. M., Bidigare R. R., Björkman K. M., Church M. J., Dore J. E. and White A. E. (2021) Seasonal-to-decadal scale variability in primary production and particulate matter export at Station ALOHA. *Progr. Oceanogr.*
- Kersten M., Kriewis M. and Förstner U. (1991) Partitioning of trace metals released from polluted marine aerosols in coastal seawater. *Mar. Chem.* **36**, 165–182.
- Kim I. N., Lee K., Gruber N., Karl D. M., Bullister J. L., Yang S. and Kim T. W. (2014) Increasing anthropogenic nitrogen in the North Pacific Ocean. *Science* **346**, 1102–1106.
- Köbberich M. and Vance D. (2017) Kinetic control on Zn isotope signatures recorded in marine diatoms. *Geochim. Cosmochim. Acta* **210**, 97–113.
- Köbberich M. and Vance D. (2018) Zinc association with surface-bound iron-hydroxides on cultured marine diatoms: A zinc stable isotope perspective. *Mar. Chem.* **202**, 1–11.
- Lemaitre N., de Souza G. F., Archer C., Wang R.-M., Planquette H., Sarthou G. and Vance D. (2020) Pervasive sources of isotopically light zinc in the North Atlantic Ocean. *Earth Planet. Sci. Lett.* **539** 116216.
- Liao W.-H. and Ho T.-Y. (2018) Particulate Trace Metal Composition and Sources in the Kuroshio Adjacent to the East China Sea: The Importance of Aerosol Deposition. *J. Geophys. Res. Oceans* **123**, 6207–6223.
- Liao W.-H. The impact of anthropogenic aerosol on trace metal cycling in the Northwestern Pacific Ocean. Ph. D. thesis, Nat. Cent. Univ., Taiwan, 2019 <https://etd.lib.nctu.edu.tw/cgi-bin/g32/ncugswb.cgi?o=dnucudr&s=id=%22GC101626014%22.&searchmode=basic>.
- Liao W.-H., Yang S.-C. and Ho T.-Y. (2017) Trace metal composition of size-fractionated plankton in the Western Philippine Sea: The impact of anthropogenic aerosol deposition. *Limnol. Oceanogr.* **62**, 2243–2259.
- Liao W. H., Takano S., Yang S. C., Huang K. F., Sohrin Y. and Ho T. Y. (2020) Zn Isotope Composition in the Water Column of the Northwestern Pacific Ocean: The Importance of External Sources. *Global Biogeochem. Cycles* **34**.
- Lim B. and Jickells T. D. (1990) Dissolved, particulate and acid-leachable trace metal concentrations in North Atlantic precipitation collected on the Global Change Expedition. *Global Biogeochem. Cycles* **4**, 445–458.
- Lim B., Jickells T. D., Colin J. L. and Losno R. (1994) Solubilities of Al, Pb, Cu, and Zn in rain sampled in the marine environment over the North Atlantic Ocean and Mediterranean Sea. *Global Biogeochem. Cycles* **8**, 349–362.
- Lin I. I., Chen J.-P., Wong G. T. F., Huang C.-W. and Lien C.-C. (2007) Aerosol input to the South China Sea: Results from the MODerate Resolution Imaging Spectro-radiometer, the Quick Scatterometer, and the Measurements of Pollution in the Troposphere Sensor. *Deep Sea Res. Part II* **54**, 1589–1601.
- Lin Y.-C., Chen J.-P., Ho T.-Y. and Tsai I. C. (2015) Atmospheric iron deposition in the northwestern Pacific Ocean and its adjacent marginal seas: The importance of coal burning. *Global Biogeochem. Cycles* **29**, 138–159.
- Little S. H., Vance D., Walker-Brown C. and Landing W. M. (2014) The oceanic mass balance of copper and zinc isotopes, investigated by analysis of their inputs, and outputs to ferromanganese oxide sediments. *Geochim. Cosmochim. Acta* **125**, 673–693.
- Liu K. K., Wang L. W., Dai M., Tseng C. M., Yang Y., Sui C. H., Oey L., Tseng K. Y. and Huang S. M. (2013) Inter-annual variation of chlorophyll in the northern South China Sea observed at the SEATS Station and its asymmetric responses to climate oscillation. *Biogeosciences* **10**, 7449–7462.
- Liu Z., Zhao Y., Colin C., Statterger K., Wiesner M. G., Huh C.-A., Zhang Y., Li X., Sompongchaiyakul P., You C.-F., Huang C.-Y., Liu J. T., Siringan F. P., Le K. P., Sathiamurthy E., Hantoro W. S., Liu J., Tuo S., Zhao S., Zhou S., He Z., Wang Y., Bunsomboonsakul S. and Li Y. (2016) Source-to-sink transport processes of fluvial sediments in the South China Sea. *Earth Sci. Rev.* **153**, 238–273.
- Losno R., Bergametti G. and Buat-Ménard P. (1988) Zinc partitioning in Mediterranean rainwater. *Geophys. Res. Lett.* **15**, 1389–1392.
- Lui H.-K., Chen K.-Y., Chen C.-T., Wang B.-S., Lin H.-L., Ho S.-H., Tseng C.-J., Yang Y. and Chan J.-W. (2018) Physical Forcing-Driven Productivity and Sediment Flux to the Deep Basin of Northern South China Sea: A Decadal Time Series Study. *Sustainability* **10**.
- Marchitto T. M., Curry W. B. and Oppo D. W. (2000) Zinc concentrations in benthic foraminifera reflect seawater chemistry. *Paleoceanography* **15**(3), 299–306.
- Maréchal C. N., Nicolas E., Douchet C. and Albarède F. (2000) Abundance of zinc isotopes as a marine biogeochemical tracer. *Geophys. Geosyst.* **1**, n/a-n/a.
- Middag R., de Baar H. J. W. and Bruland K. W. (2019) The Relationships Between Dissolved Zinc and Major Nutrients Phosphate and Silicate Along the GEOTRACES GA02 Transect in the West Atlantic Ocean. *Global Biogeochem. Cycles* **33**, 63–84.
- Moyner F., Vance D., Fujii T. and Savage P. (2017) The Isotope Geochemistry of Zinc and Copper. *Rev. Mineral. Geochem.* **82**, 543–600.
- Nriagu J. O. and Pacyna J. M. (1988) Quantitative assessment of worldwide contamination of air, water and soils by trace metals. *Nature* **333**, 134–139.

- Pacyna J. M. and Pacyna E. G. (2001) An assessment of global and regional emissions of trace metals to the atmosphere from anthropogenic sources worldwide. *Environ. Rev.* **9**, 269–298.
- Pan X., Wong G. T. F., Tai J.-H. and Ho T.-Y. (2015) Climatology of physical hydrographic and biological characteristics of the Northern South China Sea Shelf-sea (NoSoCS) and adjacent waters: Observations from satellite remote sensing. *Deep Sea Res. Part II* **117**, 10–22.
- Pichat S., Douchet C. and Albarède F. (2003) Zinc isotope variations in deep-sea carbonates from the eastern equatorial Pacific over the last 175 ka. *Earth Planet. Sci. Lett.* **210**, 167–178.
- Rosca C., Schoenberg R., Tomlinson E. L. and Kamber B. S. (2019) Combined zinc-lead isotope and trace-metal assessment of recent atmospheric pollution sources recorded in Irish peatlands. *Sci. Total Environ.* **658**, 234–249.
- Roshan S., DeVries T., Wu J. and Chen G. (2018) The Internal Cycling of Zinc in the Ocean. *Global Biogeochem. Cycles* **32**, 1833–1849.
- Roshan S., Wu J. and Jenkins W. J. (2016) Long-range transport of hydrothermal dissolved Zn in the tropical South Pacific. *Mar. Chem.* **183**, 25–32.
- Samanta M., Ellwood M. J. and Strzepek R. F. (2018) Zinc isotope fractionation by *Emiliania huxleyi* cultured across a range of free zinc ion concentrations. *Limnol. Oceanogr.* **63**, 660–671.
- Schlitzer, R., Anderson, R.F., Dodas, E.M., Lohan, M., Geibert, W., Tagliabue, A., Bowie, A., Jeandel, C., Maldonado, M.T., Landing, W.M., Cockwell, D., Abadie, C., Abouchami, W., Achterberg, E.P., Agather, A., Aguiar-Islas, A., van Aken, H. M., Andersen, M., Archer, C., Auro, M., de Baar, H.J., Baars, O., Baker, A.R., Bakker, K., Basak, C., Baskaran, M., Bates, N.R., Bauch, D., van Beek, P., Behrens, M.K., Black, E., Bluhm, K., Bopp, L., Bouman, H., Bowman, K., Bown, J., Boyd, P., Boye, M., Boyle, E.A., Branell, P., Bridgestock, L., Brissebrat, G., Browning, T., Bruland, K.W., Brumsack, H.-J., Brzezinski, M., Buck, C.S., Buck, K.N., Buesseler, K., Bull, A., Butler, E., Cai, P., Mor, P.C., Cardinal, D., Carlson, C., Carrasco, G., Casacuberta, N., Casciotti, K.L., Castrillejo, M., Chamizo, E., Chance, R., Charette, M.A., Chaves, J.E., Cheng, H., Chever, F., Christl, M., Church, T.M., Closset, I., Colman, A., Conway, T.M., Cossa, D., Croot, P., Cullen, J.T., Cutter, G.A., Daniels, C., Dehairs, F., Deng, F., Dieu, H.T., Duggan, B., Dulaquais, G., Dumousséaud, C., Echeogoyen-Sanz, Y., Edwards, R.L., Ellwood, M., Fahrback, E., Fitzsimmons, J.N., Russell Flegal, A., Fleisher, M.Q., van de Flierdt, T., Frank, M., Friedrich, J., Fripiat, F., Fröllje, H., Galer, S.J.G., Gamo, T., Ganeshram, R.S., Garcia-Orellana, J., Garcia-Solsona, E., Gault-Ringold, M., George, E., Gerringa, L.J.A., Gilbert, M., Godoy, J.M., Goldstein, S.L., Gonzalez, S.R., Grissom, K., Hammerschmidt, C., Hartman, A., Hassler, C.S., Hathorne, E. C., Hatta, M., Hawco, N., Hayes, C.T., Heimbürger, L.-E., Helgoe, J., Heller, M., Henderson, G.M., Henderson, P.B., van Heuven, S., Ho, P., Horner, T.J., Hsieh, Y.-T., Huang, K.-F., Humphreys, M.P., Ishiki, K., Jacquot, J.E., Janssen, D.J., Jenkins, W.J., John, S., Jones, E.M., Jones, J.L., Kadko, D.C., Kayser, R., Kenna, T.C., Khondoker, R., Kim, T., Kipp, L., Klar, J.K., Klunder, M., Kretschmer, S., Kumamoto, Y., Laan, P., Labatut, M., Lacan, F., Lam, P.J., Lambelet, M., Lamborg, C.H., Le Moigne, F.A.C., Le Roy, E., Lechtenfeld, O.J., Lee, J.-M., Lherminier, P., Little, S., López-Lora, M., Lu, Y., Masque, P., Mawji, E., McClain, C.R., Measures, C., Mehic, S., Barraqueta, J.-L.M., van der Merwe, P., Middag, R., Mieruch, S., Milne, A., Minami, T., Moffett, J.W., Moncoiffe, G., Moore, W.S., Morris, P.J., Morton, P.L., Nakaguchi, Y., Nakayama, N., Niedermiller, J., Nishioka, J., Nishiuchi, A., Noble, A., Obata, H., Ober, S., Ohnemus, D.C., van Ooijen, J., O’Sullivan, J., Owens, S., Pahnke, K., Paul, M., Pavia, F., Pena, L.D., Peters, B., Planchon, F., Planquette, H., Pradoux, C., Puigcorbó, V., Quay, P., Queroue, F., Radic, A., Rauschenberg, S., Rehkämper, M., Rember, R., Remenyi, T., Resing, J. A., Rickli, J., Rigaud, S., Rijkenberg, M.J.A., Rintoul, S., Robinson, L.F., Roca-Martí, M., Rodellas, V., Roeske, T., Rolison, J.M., Rosenberg, M., Roshan, S., Rutgers van der Loeff, M.M., Ryabenko, E., Saito, M.A., Salt, L.A., Sanial, V., Sarthou, G., Schallenberg, C., Schauer, U., Scher, H., Schlosser, C., Schnetger, B., Scott, P., Sedwick, P.N., Semiletov, I., Shelley, R., Sherrell, R.M., Shiller, A.M., Sigman, D. M., Singh, S.K., Slagter, H.A., Slater, E., Smethie, W.M., Snaith, H., Sohrin, Y., Soht, B., Sonke, J.E., Speich, S., Steinfeldt, R., Stewart, G., Stichel, T., Stirling, C.H., Stutsman, J., Swarr, G.J., Swift, J.H., Thomas, A., Thorne, K., Till, C.P., Till, R., Townsend, A.T., Townsend, E., Tuerena, R., Twining, B.S., Vance, D., Velazquez, S., Venchiarutti, C., Villa-Alfageme, M., Vivancos, S.M., Voelker, A.H.L., Wake, B., Warner, M.J., Watson, R., van Weerlee, E., Alexandra Weigand, M., Weinstein, Y., Weiss, D., Wisotzki, A., Woodward, E.M.S., Wu, J., Wu, Y., Wuttig, K., Wyatt, N., Xiang, Y., Xie, R.C., Xue, Z., Yoshikawa, H., Zhang, J., Zhang, P., Zhao, Y., Zheng, L., Zheng, X.-Y., Zieringer, M., Zimmer, L. A., Ziveri, P., Zunino, P. and Zurbrugg, C. (2018) The GEOTRACES Intermediate Data Product 2017. *Chem. Geol.* **493**, 210–223.
- Shelley R. U., Landing W. M., Ussher S. J., Planquette H. and Sarthou G. (2018) Regional trends in the fractional solubility of Fe and other metals from North Atlantic aerosols (GEOTRACES cruises GA01 and GA03) following a two-stage leach. *Biogeosciences* **15**, 2271–2288.
- Shiller A. M. and Boyle E. (1985) Dissolved zinc in rivers. *Nature* **317**, 49–52.
- Sholkovitz E. R., Sedwick P. N., Church T. M., Baker A. R. and Powell C. F. (2012) Fractional solubility of aerosol iron: Synthesis of a global-scale data set. *Geochim. Cosmochim. Acta* **89**, 173–189.
- Siebert C., Nögler T. F. and Kramers J. D. (2001) Determination of molybdenum isotope fractionation by double-spike multicollector inductively coupled plasma mass spectrometry. *Geochem. Geophys. Geosyst.* **2**, n/a-n/a.
- Takano S., Liao W.-H., Tian H.-A., Huang K.-F., Ho T.-Y. and Sohrin Y. (2020) Sources of particulate Ni and Cu in the water column of the northern South China Sea: Evidence from elemental and isotope ratios in aerosols and sinking particles. *Mar. Chem.* **219**.
- Takano S., Tanimizu M., Hirata T., Shin K.-C., Fukami Y., Suzuki K. and Sohrin Y. (2017) A simple and rapid method for isotopic analysis of nickel, copper, and zinc in seawater using chelating extraction and anion exchange. *Anal. Chim. Acta* **967**, 1–11.
- Tan S., Zhang J., Li H., Sun L., Wu Z., Wiesner M. G., Zheng H. and Chen J. (2020) Deep Ocean Particle Flux in the Northern South China Sea: Variability on Intra-Seasonal to Seasonal Timescales. *Frontiers in Earth Science* **8**.
- Tréguer P. J. and De La Rocha C. L. (2013) The world ocean silica cycle. *Ann. Rev. Mar. Sci.* **5**, 477–501.
- Tseng C.-M., Wong G. T.-F., Lin I.-I., Wu C.-R. and Liu K.-K. (2005) A unique seasonal pattern in phytoplankton biomass in low-latitude waters in the South China Sea. *Geophys. Res. Lett.* **32**.
- Vance D., de Souza G. F., Zhao Y., Cullen J. T. and Lohan M. C. (2019) The relationship between zinc, its isotopes, and the major nutrients in the North-East Pacific. *Earth Planet. Sci. Lett.* **525**.

- Vance D., Little S. H., Archer C., Cameron V., Andersen M. B., Rijkenberg M. J. A. and Lyons T. W. (2016) The oceanic budgets of nickel and zinc isotopes: the importance of sulfidic environments as illustrated by the Black Sea. *Philos. Trans. A Math. Phys. Eng. Sci.* **374**.
- Vance D., Little Susan H., de Souza Gregory F., Khatiwala S., Lohan Maeve C. and Middag R. (2017) Silicon and zinc biogeochemical cycles coupled through the Southern Ocean. *Nat. Geosci.* **10**, 202–206.
- Wang R., Balkanski Y., Boucher O., Bopp L., Chappell A., Ciais P., Hauglustaine D., Peñuelas J. and Tao S. (2015) Sources, transport and deposition of iron in the global atmosphere. *Atmos. Chem. Phys.* **15**, 6247–6270.
- Wang B.-S. and Ho T.-Y. (2020) Aerosol Fe cycling in the surface water of the Northwestern Pacific ocean. *Prog. Oceanogr.* **183**.
- Weber T., John S., Tagliabue A. and DeVries T. (2018) Biological uptake and reversible scavenging of zinc in the global ocean. *Science* **361**, 72–76.
- Wen L.-S., Jiann K.-T. and Santschi P. H. (2006) Physicochemical speciation of bioactive trace metals (Cd, Cu, Fe, Ni) in the oligotrophic South China Sea. *Mar. Chem.* **101**, 104–129.
- Wen Y., Yang Z. and Xia X. (2013) Dissolved and particulate zinc and nickel in the Yangtze River (China): Distribution, sources and fluxes. *Appl. Geochem.* **31**, 199–208.
- Witt M. L. I., Mather T. A., Baker A. R., De Hoog J. C. M. and Pyle D. M. (2010) Atmospheric trace metals over the south-west Indian Ocean: Total gaseous mercury, aerosol trace metal concentrations and lead isotope ratios. *Mar. Chem.* **121**, 2–16.
- Wong G. T. F., Tseng C.-M., Wen L.-S. and Chung S.-W. (2007) Nutrient dynamics and N-anomaly at the SEATS station. *Deep Sea Res. Part II* **54**, 1528–1545.
- Yang S.-C., Lee D.-C. and Ho T.-Y. (2012) The isotopic composition of Cadmium in the water column of the South China Sea. *Geochim. Cosmochim. Acta* **98**, 66–77.
- Zhang J., Li H., Xuan J., Wu Z., Yang Z., Wiesner M. G. and Chen J. (2019) Enhancement of Mesopelagic Sinking Particle Fluxes Due to Upwelling, Aerosol Deposition, and Monsoonal Influences in the Northwestern South China Sea. *J. Geophys. Res. Oceans* **124**, 99–112.
- Zheng L., Minami T., Takano S., Ho T. Y. and Sohrin Y. (2021) Sectional Distribution Patterns of Cd, Ni, Zn, and Cu in the North Pacific Ocean: Relationships to Nutrients and Importance of Scavenging. *Global Biogeochem. Cycles*. doi.10.1029/2020GB006558.
- Zhou Q., Yang N., Li Y., Ren B., Ding X., Bian H. and Yao X. (2020) Total concentrations and sources of heavy metal pollution in global river and lake water bodies from 1972 to 2017. *Global Ecol. Conserv.* **22**.

Associate Editor: Claudine Stirling